THE UNIVERSITY OF CALGARY

A KALMAN FILTER-SMOOTHER FOR AN INERTIAL SURVEY SYSTEM OF LOCAL LEVEL TYPE

by

RICHARD VOON CHOONG WONG

A THESIS

SUBMITTED TO THE FACULTY OF GRADUATE STUDIES

IN PARTIAL FULFILLMENT OF THE REQUIREMENTS FOR THE DEGREE OF

MASTER OF SCIENCE IN ENGINEERING

DEPARTMENT OF CIVIL ENGINEERING

Division of Surveying Engineering

CALGARY, ALBERTA

SEPTEMBER 1982

ABSTRACT

The research reported in this thesis investigates the suitability of Kalman filtering and optimal smoothing for the data measured by the Ferranti Inertial Land Surveyor (FILS). The development of such a filter-smoother consists of four major steps. First the dynamics matrix for the system of interest is derived from the general error equation of a local level inertial survey system (LLISS). The next step is the derivation of the transition matrix either by analytical or numerical methods for the propagation of the state errors. The third step is the implementation of the Kalman filtering and backward smoothing equations. The final step is the testing of the Kalman filter-smoother with actual data and the assessment of the correctness of initial variances and error assumptions.

Results of this research show that Kalman filtering and optimal smoothing is a viable alternative to the method used, at present, in the FILS-software. It provides not only the coordinates but also their estimated accuracy. The filter can be modified for real-time applications and can be used to integrate the LLISS with other surveying systems. The Kalman filter-smoother was tested with inertial survey data gathered over a 42 km L-shaped base line near Calgary. Analysis of the results indicates that coordinates can be determined with sub-metre (1σ) accuracy, which is about the same as the accuracy of the control coordinates of the base line.

ACKNOWLEDGEMENTS

The author would like to thank his supervisor, Dr. Klaus-Peter Schwarz, for his advice and guidance, which were important to the completion of this research. Thanks are due to Dr. E.J. Krakiwsky, Dr. R.J. Brown, and Dr. C.S. Fraser for their critique and constructive comments regarding this work. Mr. Alex Hittel and John Hagglund of Sheltech Canada are acknowledged for providing the test data and information on the Ferranti Inertial Land Surveyor. Thanks are also due to Mrs. Mona Tod for her patience and assistance in the typing and final preparation of this thesis.

This research was partially supported by a Natural Science and Engineering Research Postgraduate Scholarship, by the JMR Research Award in 1981 and by financial assistance provided by the Geodetic Survey of Canada.

TABLE OF CONTENTS

LIST OF TABLES

LIST OF FIGURES

Notations

Frequently used notations in this thesis are listed below:

ϕ - geodetic latitude

λ - geodetic longitude

h - height

$\dot{}$ - time derivative

i - quantity in the inertial system

e - quantity in the average geodetic system

$\ell\ell$ - quantity in the local level system

p - quantity in the platform system

a - quantity in the accelerometer system

C_i^j - matrix that transforms quantities from the i-system to the j-system

ω_{ij}^m - angular velocity of the j-system with respect to the i-system coordinatized in the m-system

Ω_{ij}^k - skew systematic matrix of ω_{ij}^k

ω_e - earth rate of rotation (rad/s)

ℓ - $(\dot{\lambda} + \omega_e)$

r - mean radius of the earth

γ - normal gravity

f - specific force $(m \cdot s^{-2})$

η - east component of the deflection of the vertical (rad.)

ξ - north component of the deflection of the vertical (rad.)

Δg - gravity anomaly $(m \cdot s^{-2})$

F - dynamics matrix

Φ - transition matrix

x - state vector

P - variance matrix of the state vector

H - design matrix

K - Kalman gain matrix

y - observation noise in the control measurements

R - variance matrix of the control measurements

χ - a state vector, used in smoothing as an intermediate quantity

X - variance matrix of χ

$\hat{}$ - symbolizes a measured quantity

$\tilde{}$ - symbolizes a computed quantity

(-) - symbolizes quantities before update

(+) - symbolizes quantities after update

^{s} - symbolizes quantities after smoothing

δ - symbolizes the error in a quantity

Chapter 1

INTRODUCTION

In recent years, inertial survey systems have become one of the widely used surveying devices in Canada. Many difficult surveying tasks that were previously carried out with conventional survey tools can now be accomplished in much less time with an inertial survey system. The cost of inertial surveys, in both ground vehicle and helicopter modes, can be as low as one-half of the cost of the conventional survey methods (Babbage, 1977; 1981). Ordinarily, these systems can give geodetic positions with second-order or higher accuracy if proper estimation techniques are employed to determine the error states of the systems (Schwarz, 1980a).

There are three types of inertial survey systems: space stabilized, local level, and strapdown. In all three system types the major sensors are the three orthogonal accelerometers. The accelerometers measure the specific force acting on the system. From the sensed forces, the accelerations of the system are computed and integrated mechanically into velocities which are then integrated into changes in position of the system by the on board computer. The integrated velocity information is also used by the computer to control the gyros that align the platform of the system. The three types of inertial survey systems mentioned above are distinguished by the manner in which they control their platform. In the space stabilized system, the three orthogonal axes of the platform are kept

by the gyros in fixed orientations with respect to an inertial coordinate system. The local level system has a platform perpendicular to the local normal of the reference ellipsoid. One of its horizontal axes is always pointing towards north. The strapdown system follows all movements of the vehicle. The platform rotations are sensed and taken into account computationally, therefore, the system needs a much more powerful computer than the other types of system. The final outputs from these inertial systems are usually geodetic curvilinear coordinates. Details on the mechanizations of these systems can be found in Britting (1971).

The system of interest in this research is the local level inertial survey system (LLISS). Systems of this type available in Canada are the Litton Autosurveyor (ISS) and the Ferranti Inertial Land Surveyor (FILS). At present, the manufacturer of the ISS supplies an estimation package that contains a Kalman filter. This package is built into the system therefore the model for the Kalman filter is difficult to determine. The FILS predicts its position errors with a quadratic polynomial fitting technique (Deren and Hagglund, 1981). The prediction technique does not provide to the user the variances of the predicted coordinates. Also, neither of these two systems uses the linear optimal smoothing technique to process their data post-mission. The objectives of this research are the development of an optimal Kalman filter-smoother for the FILS, and the implementation of the optimal equations for computing the cross-variances between the coordinates of the different points in the

same mission after filtering.

Most of the error models, as well as the Kalman filtering and smoothing equations used in this thesis can be found in the literature on inertial navigation and linear optimal estimation, e.g. Britting (1971) and Gelb (1974). The adaptation of these general equations to the specific case of an LLISS is the major concern in this thesis. This includes the formulation of the transition matrix and the application of Kalman filtering and optimal smoothing equations in estimating the error states of the FILS with velocity errors and known coordinate control measurements. Tests of the derived filter-smoother are done with the FILS data gathered at an L-shaped base line where accurate coordinates are available for comparison.

In order to clarify the error equations used in this research, Chapter 2 is devoted to the definitions of the different coordinate systems and the transformations that relate the quantities measured by an LLISS to an inertial coordinate system. Chapters 3 and 4 deal with the derivation of the dynamics and transition matrices, and Chapter 5 lists the Kalman filtering and backward smoothing equations and discusses their implementation. The results of the tests, the error analysis and recommendations are given in the last two chapters of this thesis.

Chapter 2

COORDINATE SYSTEMS

The sensors in the LLISS are aligned to a locally defined geodetic system which is topocentric in nature. The measurements and computations are performed in this local level geodetic frame. The coordinates most users require are referred to a geodetic ellipsoid (geodetic system) which can be linked to the right ascension system. Theoretically, the right ascension system is not inertial because it moves with respect to the distant galaxies. Ignoring such movement will introduce errors of the order of $2 \cdot 10^{-8}$ deg/hr (Kayton, 1961) which is about 5 orders of magnitude higher than the accuracy of the sensors in the LLISS. Therefore, for all practical purposes, it can be regarded as an inertial system. The conversion of the quantities determined by the LLISS to the geodetic system involves a series of transformation through several different coordinate systems. These transformations and the definitions of the different coordinate systems dictate the formulation of the error models of the LLISS. There are several definitions of local level coordinate systems in the literature on inertial survey error analysis. To avoid any confusion of the error equations given in the next chapter with other similar equations, all the coordinate systems used in this research are defined here in point form.

2.1 Inertial System (i)

(i) 3-D Cartesian frame

(ii) Heliocentric

(iii) Tertiary axis passes through the north celestial pole

(iv) Primary axis passes through the vernal equinox

(v) Right-handed.

2.2 Average Geocentric System (e)

(i) 3-D Cartesian frame

(ii) Geocentric

(iii) Tertiary axis coincides with earth mean spinning axis

(iv) Primary axis is the intersection of the Greenwich meridian and the equator

(v) Right-handed.

2.3 Local Level System (ℓℓ)

(i) 3-D Cartesian frame

(ii) Origin at the system location

(iii) Tertiary axis orthogonal to the reference ellipsoid and pointing outward

(iv) Primary axis pointing east

(v) Right-handed.

Figure 2-1 shows the relationship between the average geocentric and local level system.

2.4 Platform system (p)

For error analysis purposes, the platform system can be defined in two ways. Its axes can be assumed orthogonal and linked to the accelerometer axes by their angular non-orthogonalities, or they can be treated as coincident with the accelerometer axes. The FILS corrects for the non-orthogonalities of its accelerometers,

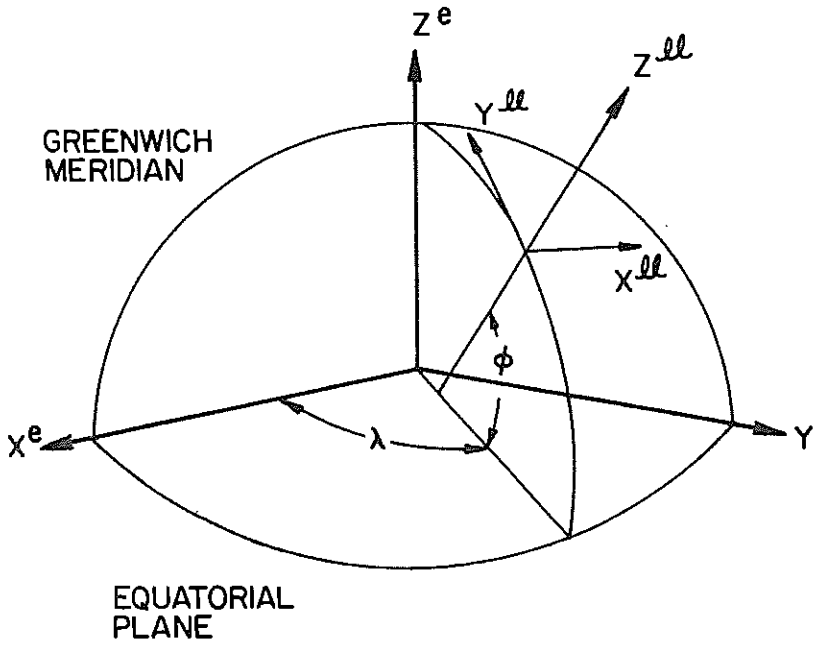

Figure 2-1 : Relationship between average geocentric and local level systems

therefore the former case is adopted here. The platform system is defined as

(i) 3-D Cartesian frame,

(ii) origin is the same as the ℓℓ-system,

(iii) all axes are assumed to be aligned with the corresponding axes of the local level system and

(iv) right-handed.

Mathematically, the quantities in the ℓℓ-system can be transformed to the e-system with the well known matrix

$$C^{e}_{\ell\ell} = \begin{bmatrix} \cos\lambda & -\sin\phi\sin\lambda & \cos\phi\sin\lambda \\ \sin\lambda & \sin\phi\cos\lambda & -\cos\phi\cos\lambda \\ 0 & \cos\phi & \sin\phi \end{bmatrix} , \qquad (2\text{-}1)$$

see Vanicek and Krakiwsky (1982). Here, ϕ and λ are the geodetic latitude and longitude of the LLISS. The transformation matrix between the average geocentric and the inertial system is

$$C^{i}_{e} = \begin{bmatrix} \cos(\omega_e t + \text{GAST}) & -\sin(\omega_e t + \text{GAST}) & 0 \\ \sin(\omega_e t + \text{GAST}) & \cos(\omega_e t + \text{GAST}) & 0 \\ 0 & 0 & 1 \end{bmatrix} , \qquad (2\text{-}2)$$

where ω_e is the constant angular velocity of the earth (for small t),

t is the elapsed time since the beginning of the mission and

GAST is the Greenwich Apparent Siderial Time at $t = 0$.

For error analysis purposes, GAST can be chosen to be zero.

The angular velocity of the local level system (designated by subscript $\ell\ell$) with respect to the inertial system coordinatized in the local level system (designated by superscript $\ell\ell$) is

$$\omega^{\ell\ell}_{i\,\ell\ell} = \{-\dot{\phi},\ \ell\cos\phi,\ \ell\sin\phi\}^{T} , \qquad (2\text{-}3)$$

where

$$\ell = \omega_e + \dot{\lambda} . \qquad (2\text{-}4)$$

This relation is shown in Figure 2-2.

Expressing the angular velocity of the earth with respect to the inertial frame in the local level system, yields

$$\omega^{\ell\ell}_{i\,e} = \{0,\ \omega_e\cos\phi,\ \omega_e\sin\phi\}^{T} . \qquad (2\text{-}5)$$

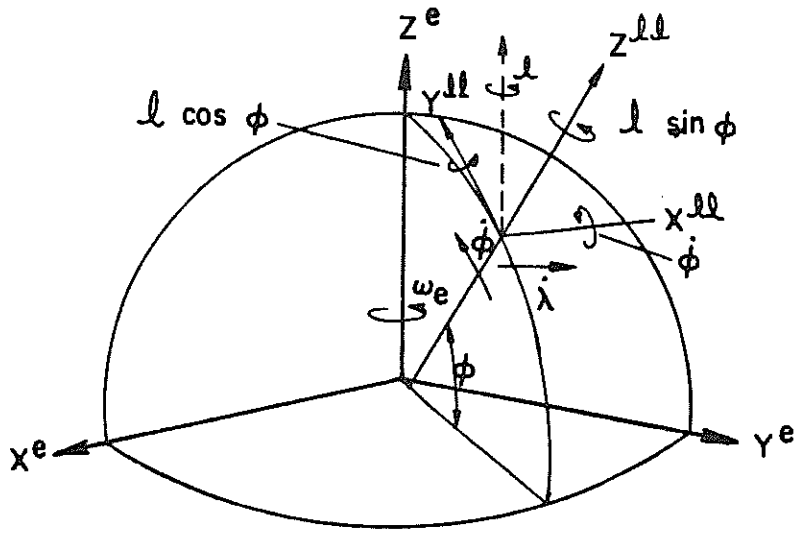

Figure 2-2 : Angular Rotation of the Local Level System

The difference between equations (2-3) and (2-5) is the angular velocity

$$\omega_{e\,ll}^{ll} = \{-\dot{\phi},\ \dot{\lambda}\cos\phi,\ \dot{\lambda}\sin\phi\}^T \quad . \tag{2-6}$$

The derivations of the LLISS error equations in the next chapter involve taking the cross products of these vectors with other quantities. In order to simplify this kind of operation, the following equivalence is used

$$\omega \times r = \Omega r \quad , \tag{2-7}$$

where Ω is the skew symmetric matrix of the angular velocity vector ω. The skew symmetric matrices of the two angular velocities $\omega_{i\,e}^{ll}$ and $\omega_{e\,ll}^{ll}$ are

$$\Omega_{ie}^{\ell\ell} = \begin{bmatrix} 0 & -\omega_e \sin\phi & \omega_e \cos\phi \\ \omega_e \sin\phi & 0 & 0 \\ -\omega_e \cos\phi & 0 & 0 \end{bmatrix}, \qquad (2\text{-}8)$$

and

$$\Omega_{e\,\ell\ell}^{\ell\ell} = \begin{bmatrix} 0 & -\dot{\lambda} \sin\phi & \dot{\lambda} \cos\phi \\ \dot{\lambda} \sin\phi & 0 & \dot{\phi} \\ -\dot{\lambda} \cos\phi & -\dot{\phi} & 0 \end{bmatrix}. \qquad (2\text{-}9)$$

The addition of the two matrices yields

$$\Omega_{i\,\ell\ell}^{\ell\ell} = \begin{bmatrix} 0 & -\ell \sin\phi & \ell \cos\phi \\ \ell \sin\phi & 0 & \dot{\phi} \\ -\ell \cos\phi & -\dot{\phi} & 0 \end{bmatrix}. \qquad (2\text{-}10)$$

2.5 Accelerometer System (a)

The accelerometer system is another system that should be mentioned here. The three accelerometers of the LLISS together form a coordinate frame that has the following characteristics:

(i) the origin is the intersection of the accelerometer axes,

(ii) the axes are usually non-orthogonal and

(iii) it is upright and right-handed.

If the six angular deviations between the accelerometer and platform axes are small, the non-orthogonal transformation from the accelerometer system to the orthogonal platform system can be expressed in the general form (Britting, 1971)

$$C_a^p = I + \Delta C_a^p \quad , \tag{2-11}$$

where

$$\Delta C_a^p = \begin{bmatrix} 0 & -\theta_{yz} & \theta_{zy} \\ \theta_{xz} & 0 & -\theta_{zx} \\ -\theta_{xy} & \theta_{yx} & 0 \end{bmatrix} \quad . \tag{2-12}$$

The small angle θ_{ij} is the component of the angular deviation between the i and j axes along the direction of the third axis. These angles in the FILS are regularly determined from calibration data. They are treated as known and constant between calibrations.

Chapter 3

ERROR EQUATIONS

Due to the imperfections in the instruments and the alignment of the system, the geodetic measurements given by the LLISS are always contaminated by both systematic and random errors. Under normal conditions, the same type of systematic and random errors are present in the system. Constant system errors can be accurately removed by regular calibrations. The errors that are random from mission to mission but are systematic during the same mission are known as state errors. These errors in the sensors induce errors in the integrated velocities and position coordinates which are, in turn, used to command the gyros. Thus, the state errors have an interwoven relationship with each other. For a first order error analysis, this relationship can be mathematically described by a set of linear differential equations that expresses the time rate of change of these state errors. This chapter is devoted to the derivation of this set of equations.

3.1 Error Sources

The system errors in the LLISS can be identified by looking into the different sources of error. The accelerometers measure the specific force that acts on the system. The instruments are imperfect, therefore the accelerations determined from the measurements given by

accelerometers are usually biased. The instrument errors and uncertainties in the predicted velocities and positions make it very difficult to align the platform perfectly with the local level frame. The misalignments introduce errors into the measured components of the specific force. The accelerometers are designed to sense any forces regardless of their source, therefore the sensed forces contain the accelerations of the vehicle with respect to the inertial frame as well as gravitational attraction. The accelerations cannot be accurately determined unless the gravity field along the survey line is known. Since we do not have such information prior to a survey, the normal gravity field is usually chosen as a first approximation. This approximation is another source of error if the gravity disturbances on the survey line are large. For a more detailed discussion of these errors, see Britting (1971) and Schwarz (1978, 1980c).

3.1.1 Acceleration Error Equations

The specific force equation for an LLISS is well documented, e.g. Britting (1971) and Herrewegen (1980). The equation coordinatized in the local level system is

$$f^{\ell\ell} = \dot{v}^{\ell\ell} + (\Omega^{\ell\ell}_{e\,\ell\ell} + 2\Omega^{\ell\ell}_{i\,e})\, v^{\ell\ell} - g^{\ell\ell} \quad . \tag{3-1}$$

Here, $f^{\ell\ell}$ is the specific force vector, v is the velocity vector and g is the gravity vector. For a first order error analysis, the velocity vector of the system can be written as

$$\begin{bmatrix} v_N \\ v_E \\ v_U \end{bmatrix}^{\ell\ell} = \begin{bmatrix} r\,\dot{\lambda}\cos\phi \\ r\,\dot{\phi} \\ \dot{h} \end{bmatrix} , \tag{3-2}$$

where r is the mean radius of the earth and h is the ellipsoidal height. The acceleration error equation for the LLISS can be derived by taking the total differential of equation (3-1) and then ordering with respect to $\delta\dot{v}^{\ell\ell}$. The result is

$$\delta\dot{v}^{\ell\ell} = \delta f^{\ell\ell} - (\Omega^{\ell\ell}_{e\,\ell\ell} + 2\Omega^{\ell\ell}_{i\,e})\,\delta v^{\ell\ell} + v^{\ell\ell}(\delta\omega^{\ell\ell}_{e\,\ell\ell} + 2\omega^{\ell\ell}_{i\,e}) + \delta g^{\ell\ell} , \tag{3-3}$$

where δ symbolizes errors. Equation (3-3) shows that the errors in the accelerations determined by the system are a function of the measured specific force, the gravity disturbances, the velocities and the computed angular velocity vectors. The specific force measurements contain instrument errors and errors incurred by the misalignment of the platform. If the non-orthogonality of the accelerometers are not compensated for, then the outputs of the accelerometers in the platform system are

$$\hat{f}^P = f^P + (\Delta C^P_a)^T f^P + S_a f^a + (u) f^a , \tag{3-4}$$

where ΔC^P_a is defined by (2-12),

$\hat{}$ symbolizes the measured quantities,

S_a is the scale factor matrix and

and $(u) f^a$ is the white or coloured noise.

Due to the different errors in the gyros and their torquing commands, the inertial platform is misaligned with respect to the local level

system. The three angular misalignments between axes of the two systems are called the attitude or misalignment errors. They are denoted by

$$\{\varepsilon_E,\ \varepsilon_N,\ \varepsilon_U\}^{\ell\ell} \quad , \tag{3-5}$$

where

ε_E is the misalignment of the east axis,

ε_N is the misalignment of the north axis, and

ε_U is the misalignment of the vertical axis.

The outputs of the accelerometers given in the equation (3-4) can be transformed to the local level system by use of the transform matrix

$$C_p^{\ell\ell} = I + E^{\ell\ell} \quad , \tag{3-6}$$

where

$$E^{\ell\ell} = \begin{bmatrix} 0 & -\varepsilon_U & \varepsilon_N \\ \varepsilon_U & 0 & -\varepsilon_E \\ -\varepsilon_N & \varepsilon_E & 0 \end{bmatrix} \quad . \tag{3-7}$$

Since the system assumes that the platform is perfectly aligned with the local level frame, the sensed specific force coordinatized in the $\ell\ell$-frame becomes (Britting, 1971)

$$\hat{f}^{\ell\ell} = f^p + (\Delta C_a^p)^T f^p + S_a f^a + (u) f^a \quad . \tag{3-8}$$

Since

$$f^p = (I - E)^{\ell\ell} f^{\ell\ell} \quad , \tag{3-9}$$

the sensed force can be rewritten as

$$\hat{f}^{\ell\ell} = f^{\ell\ell} - \{E^{\ell\ell} f^{\ell\ell} + (\Delta C_a^p)^T f^{\ell\ell} + S_a f^a + (u) f^a\} + \delta g^{\ell\ell} \quad . \tag{3-10}$$

The terms in the bracket in equation (3-10), represent the error $\delta f^{\ell\ell}$ in equation (3-3).

The vector $\delta g^{\ell\ell}$ in equation (3-3) is the difference between the normal gravity vector

$$\gamma^{\ell\ell} = \begin{bmatrix} 0 \\ 0 \\ -\gamma_o + \frac{\partial \gamma}{\partial h} h \end{bmatrix} , \qquad (3\text{-}11)$$

and the actual gravity vector

$$g^{\ell\ell} = \begin{bmatrix} \eta g \\ \xi g \\ -\gamma_o - \Delta g \end{bmatrix} , \qquad (3\text{-}12)$$

where

γ_o is the normal gravity on the reference ellipsoid,

h is the height above the ellipsoid,

η is the east component of the deflection of the vertical,

ξ is the north component of the deflection of the vertical and

Δg is the gravity anomaly.

Using the normal gravity as a good approximation to the value of g, the errors caused by the gravity disturbances can be rewritten as

$$\delta g^{\ell\ell} = \begin{bmatrix} \eta\gamma \\ \xi\gamma \\ -\frac{\partial \gamma}{\partial h} \delta h - \Delta g \end{bmatrix} . \qquad (3\text{-}13)$$

This equation shows that the height state error has a very strong effect on the accuracy of the vertical velocity if the uncorrected height is used to compute the normal gravity. This effect may be dampened if the state error of the uncorrected height is both predicted in real-time and used in the computation of the normal gravity. In some air-borne applications, external height information is available. In that case, the normal gravity can be computed with a weighted mean value of the uncorrected and the external height, (h_o, h_{ex}) (see Britting, 1971). If the mean height is computed by the formula

$$h_m = h_o^{(1-\alpha)} \cdot h_{ex}^{\alpha} \quad , \tag{3-14}$$

where α is the weighting factor, then

$$\delta g^{\ell\ell} = \begin{bmatrix} \eta\gamma \\ \xi\gamma \\ -\frac{2\gamma(1-\alpha)}{r}\,\delta h + \Delta g \end{bmatrix} \quad . \tag{3-15}$$

Thus equation (3-3) may be rewritten in terms of the known errors as

$$\dot{\delta v}^{\ell\ell} = -Ef^{\ell\ell} - (\Omega_{e\,\ell\ell}^{\ell\ell} + 2\Omega_{i\,e}^{\ell\ell})\,\delta v^{\ell\ell} + v^{\ell\ell}(\delta\omega_{i\,\ell\ell}^{\ell\ell} + 2\delta\omega_{i\,e}^{\ell\ell}) + \delta g^{\ell\ell} + (\Delta C_a^p)^T f^{\ell\ell} + S_a f^a + (u) f^a \quad . \tag{3-16}$$

3.1.2 Attitude Error Equations

The angular misalignment between the axes of the inertial platform and the local level system are caused by the errors in the

computer commands that steer the gyros, by the gyro biases and the noise in the devices themselves. Descriptions of the different kinds of biases in various types of gyro mechanization can be found in Savage (1978). For a first order error analysis, the sum of all biases is usually treated as being constant. Its influence on the computed coordinates is a systematic function of time. The errors in the computer commands are caused by the inaccuracies, i.e. state errors, in the integrated velocities and positions given by the LLISS. The influences of these errors on the angular velocities between the inertial system and the local level system can be analyzed in the following way.

In the local level system, we have

$$\delta\omega^{\ell\ell}_{i\,\ell\ell} = \tilde{\omega}^{\ell\ell}_{i\,\ell\ell} - \omega^{\ell\ell}_{i\,\ell\ell} \quad , \tag{3-17}$$

where $\tilde{}$ symbolizes a computed quantity. Due to the biases in the gyros and $\delta\omega^{\ell\ell}_{i\,\ell\ell}$, the actual angular velocity between the platform and the inertial system coordinatized in the platform system may be written as

$$\omega^{p}_{i\,p} = \omega^{\ell\ell}_{i\,\ell\ell} + \delta\omega^{p}_{i\,p} \quad , \tag{3-18}$$

where $\delta\omega^{p}_{i\,p}$ is the total platform angular velocity error. The biases which include the gyro scale errors and the misalignment of gyro axes are commonly grouped together and are called gyro drift. Denoting the drift as δd, the error $\delta\omega^{p}_{i\,p}$ can be expressed by the equation

$$\delta\omega^{p}_{i\,p} = \delta\omega^{\ell\ell}_{i\,\ell\ell} + \delta d^{\ell\ell} + (u)\ \omega^{\ell\ell}_{i\,\ell\ell} \quad . \tag{3-19}$$

Together with equation (3-17), these equations outline the sources of the attitude errors in the LLISS.

The attitude error equations for the LLISS express the time rate of change of the attitude errors by way of the time derivative of the transformation matrix $C_p^{\ell\ell}$, i.e.

$$\dot{C}_p^{\ell\ell} = C_p^{\ell\ell}\ \Omega_{\ell\ell\ p}^{p} \quad . \tag{3-20}$$

The rate of change of the corresponding angular velocity vector is

$$\dot{\omega}_{\ell\ell\ p}^{\ell\ell} = (I + E)^{\ell\ell}\ \omega_{\ell\ell\ p}^{p} \quad . \tag{3-21}$$

Replacing the $\omega_{\ell\ell\ p}^{p}$ as

$$\omega_{\ell\ell\ p}^{p} = \delta\omega_{i\ p}^{p} + E^{\ell\ell}\ \omega_{i\ \ell\ell}^{\ell\ell} \ , \tag{3-22}$$

and denoting the vector of attitude error as ε yields

$$\dot{\varepsilon}^{\ell\ell} = -\Omega_{i\ \ell\ell}^{\ell\ell}\ \varepsilon + \delta\omega_{i\ \ell\ell}^{\ell\ell} + \delta d^{\ell\ell} + (u)\ \omega_{i\ \ell\ell}^{\ell\ell} \quad . \tag{3-23}$$

A more detailed derivation of equation (3-23) can be found in Appendix A. A similar derivation is also given in Britting (1971).

Error equations (3-10), (3-15) and (3-23) describe the time rate of change of the systematic errors that dominate the error states of an LLISS. They show that there are three types of errors present in the system. The attitude, velocity and position errors form the basic state errors that must be considered in an error analysis because they change with respect to time and influence mainly the accuracies of the computed quantities in the system. The second type of error comprises the biases in the instruments. They are normally treated as time independent in a first order error analysis,but their effects on the size of the basic state errors are systematic as functions of time.

The remaining non-random errors, namely the gravity disturbances, are position dependent. Therefore they are not affected by the error state in the system and they can be determined before the survey mission.

3.2 Dynamics Matrix

The error equations given in the last section are linearized for first order error analysis. The mathematical functions involved are derived here for a more detailed analysis of the behaviour of the errors. The inter-relationship of these errors can be seen by expressing them in matrix form.

3.2.1 Attitude Error Equations in Matrix Form

To derive the attitude error equations in matrix form, they have to be treated individually. The $\delta\omega^{\ell\ell}_{i\,\ell\ell}$ term in equation (3-23) is obtained by differentiating $\omega^{\ell\ell}_{i\,\ell\ell}$ with respect to the state errors, i.e.

$$\delta\omega^{\ell\ell}_{i\,\ell\ell} = \begin{bmatrix} 0 & 0 & -1 & 0 \\ -\ell \sin\phi & 0 & 0 & \cos\phi \\ \ell \cos\phi & 0 & 0 & \sin\phi \end{bmatrix} \begin{bmatrix} \delta\phi \\ \delta\lambda \\ \delta\dot{\phi} \\ \delta\dot{\lambda} \end{bmatrix} . \qquad (3\text{-}24)$$

Substituting this equation and equation (2-9) into equation (3-23), we get

$$\begin{bmatrix} \dot{\varepsilon}_E \\ \dot{\varepsilon}_N \\ \dot{\varepsilon}_U \end{bmatrix} = \begin{bmatrix} 0 & \ell \sin\phi & -\ell \cos\phi & 0 & 0 & -1 & 0 \\ -\ell \sin\phi & 0 & -\dot{\phi} & -\ell \sin\phi & 0 & 0 & \cos\phi \\ \ell \cos\phi & \dot{\phi} & 0 & \ell \cos\phi & 0 & 0 & \sin\phi \end{bmatrix} \begin{bmatrix} \varepsilon_E \\ \varepsilon_N \\ \varepsilon_U \\ \delta\phi \\ \delta\lambda \\ \delta\dot{\phi} \\ \delta\dot{\lambda} \end{bmatrix} \qquad (3\text{-}25)$$

$$+ \delta d^{\ell\ell} + (u)\ \omega^{\ell\ell}_{i\,\ell\ell} \ .$$

3.2.2 Acceleration Error Equations in Matrix Form

Many of the terms in the acceleration error equation (3-13) have either been given or defined in previous sections. The remaining terms to be derived here are $\delta\omega^{\ell\ell}_{e\,\ell\ell}$ and $\delta\omega^{\ell\ell}_{i\,e}$. Taking the partial derivations of $\omega^{\ell\ell}_{e\,\ell\ell}$ and $\omega^{\ell\ell}_{i\,e}$, the two terms in matrix form become:

$$\delta\omega^{\ell\ell}_{e\,\ell\ell} = \begin{bmatrix} 0 & 0 & -1 & 0 \\ -\dot{\lambda} \sin\phi & 0 & 0 & \cos\phi \\ \dot{\lambda} \cos\phi & 0 & 0 & \sin\phi \end{bmatrix} \begin{bmatrix} \delta\phi \\ \delta\lambda \\ \delta\dot{\phi} \\ \delta\dot{\lambda} \end{bmatrix} , \qquad (3\text{-}26)$$

and

$$\delta\omega^{\ell\ell}_{i\,e} = \begin{bmatrix} 0 & 0 & 0 & 0 \\ -\omega_e \sin\phi & 0 & 0 & 0 \\ \omega_e \cos\phi & 0 & 0 & 0 \end{bmatrix} \begin{bmatrix} \delta\phi \\ \delta\lambda \\ \delta\dot{\phi} \\ \delta\dot{\lambda} \end{bmatrix} . \qquad (3\text{-}27)$$

In the FILS, the corrected coordinates are used to calculate the angular velocity $\omega^{\ell\ell}_{i\,\ell\ell}$. These coordinates are predicted by a built-in computer program. Their errors are much smaller than the position state errors, therefore the influences of $\delta\lambda$ and $\delta\phi$ can be neglected. After premultiplying the $\delta\omega^{\ell\ell}_{e\,\ell\ell}$ by the skew-symmetric matrix of $v^{\ell\ell}$, the third term of equation (3-16) in geodetic curvilinear coordinates can be rewritten as

$$v^{\ell\ell}(\delta\omega^{\ell\ell}_{e\,\ell\ell} + 2\delta\omega^{\ell\ell}_{i\,e}) = \begin{bmatrix} 0 & 0 & 0 & \dot{\phi}\tan\phi - \frac{\dot{h}}{r} \\ 0 & 0 & -\frac{\dot{h}}{r} & -\frac{1}{2}\dot{\lambda}\sin 2\phi \\ 0 & 0 & r\dot{\phi} & r\dot{\lambda}\cos^2\phi \end{bmatrix} \begin{bmatrix} \delta\phi \\ \delta\lambda \\ \delta\dot{\phi} \\ \delta\dot{\lambda} \end{bmatrix} . \qquad (3\text{-}28)$$

Finally, by expanding the other terms in equation (3-16), the acceleration error equations in terms of geodetic curvilinear coordinates become:

$$\begin{bmatrix} \delta\ddot{\phi} \\ \delta\ddot{\lambda} \\ \delta\ddot{h} \end{bmatrix} = \begin{bmatrix} \frac{fU}{r} & 0 & \frac{fE}{r} & 0 & 0 & 0 & -\ell\sin 2\phi & 0 & \frac{-2\dot{\phi}}{r} \\ 0 & -\frac{fN}{r}\sec\phi & \frac{fN}{r}\sec\phi & 0 & 0 & 2\ell\tan\phi & 0 & 0 & \frac{-(\dot{\lambda}+2\omega_e)}{r} \\ -fN & fE & 0 & 0 & 0 & 2r\dot{\phi} & 2r\ell\cos^2\phi & \frac{2\gamma}{r}(1-\alpha) & 0 \end{bmatrix} \begin{bmatrix} \varepsilon_E \\ \varepsilon_N \\ \varepsilon_U \\ \delta\phi \\ \delta\lambda \\ \delta\dot{\phi} \\ \delta\dot{\lambda} \\ \delta h \\ \delta\dot{h} \end{bmatrix}$$

$$+ \begin{bmatrix} \xi\gamma \\ \eta\gamma \\ \Delta g \end{bmatrix} + (\Delta C^p_a)^T f^a + S_a f^a + (u) f^a . \qquad (3\text{-}29)$$

where fE, fN and fU are specific force components in the east, north and vertical directions. The vertical velocity is eliminated because, in the ground vehicle mode, it is small compared to the horizontal velocities. Its effect on the error propagation becomes negligible compared to the other terms. A complete derivation of the acceleration error equations is given in Appendix B.

Equations (3-25) and (3-29) together form a matrix that describes the inter-relationship of the basic state errors. In the estimation literature, this matrix is commonly known as the dynamics matrix. The dynamics matrix derived here is printed in Figure 3-1. A similar matrix is also given in Schmidt (1978).

$$
F = \begin{bmatrix}
0 & \ell \sin\phi & -\ell\cos\phi & 0 & 0 & -1 & 0 & 0 & 0 \\
-\ell\sin\phi & 0 & -\dot{\phi} & -\ell\sin\phi & 0 & 0 & \cos\phi & 0 & 0 \\
\ell\cos\phi & \dot{\phi} & 0 & \ell\cos\phi & 0 & 0 & \sin\phi & 0 & 0 \\
0 & 0 & 0 & 0 & 0 & 1 & 0 & 0 & 0 \\
0 & 0 & 0 & 0 & 0 & 0 & 1 & 0 & 0 \\
fU/r & 0 & -fE/r & 0 & 0 & 0 & -\ell\sin 2\phi & & -2\dot{\phi}/r \\
0 & -fU\sec\phi/r & fN\sec\phi/r & 0 & 0 & (\dot{\lambda}+2\omega_e)\tan\phi & 0 & 0 & -(\dot{\lambda}+2\omega_e)/r \\
0 & 0 & 0 & 0 & 0 & 0 & 0 & 0 & 1 \\
-fN & fE & 0 & 0 & 0 & 2r\dot{\phi} & 2r\ell\cos^2\phi & 2\gamma/r - k2 & 0
\end{bmatrix}
$$

where $k2 = 2\alpha\ \gamma/r$ is a damping constant

Figure 3-1 : Dynamics Matrix

Chapter 4

TRANSITION MATRIX

The error equations derived in the last chapter are a set of inhomogeneous linear differential equations. Denoting the state vector as x, this set of equations becomes (Hochstadt, 1975)

$$\dot{x}(t) = F(t)\ x(t) + G(t)\ u(t) \quad , \tag{4-1}$$

with initial conditions

$$x(o) = \text{constant} \quad . \tag{4-2}$$

The term G(t) u(t) is called the forcing function and represents the unmodelled terms in equations (3-25) and (3-29) as stochastic quantities. The solution of equation (4-1) is (Gelb, 1974)

$$x(t) = \Phi(t,o)\ x(o) + \int_o^t \Phi(t,o)\ \Phi^{-1}(\tau,o)\ G(\tau)\ u(\tau)\ d\tau \quad , \tag{4-3}$$

where

$\Phi(t,o)$ is the transition matrix of the time interval of t seconds computed at o.

The complexity of equation (4-3) makes it very difficult, if not impossible, to determine an analytical solution for the LLISS. A good approximation to this solution can be obtained if the differential equations are assumed to be homogeneous, i.e. if the forcing function is assumed zero and the solution becomes

$$x(t) = \Phi(t,o)\ x(o) \quad , \tag{4-4}$$

with the transition matrix yet to be determined.

The error of this approximation is the mean of the random noise accumulated over the time interval of t seconds.

The changes of the elements in the matrix F given in Figure 3-1 over a short time interval are usually very small compared to the size of these elements. Thus, the matrix can be assumed constant over a short period of time. There are several ways to compute the transition matrix of a constant dynamics matrix. The most commonly used, simple but time consuming numerical method is the expansion of the matrix exponential

$$\Phi(t,o) = I + Ft + F^2 \frac{t^2}{2} + \ldots \qquad (4\text{-}5)$$

For application in the LLISS, the time interval may be chosen so small that the exponential can be replaced by a Taylor series truncated after the second term

$$\Phi(t,o) = I + Ft \quad . \qquad (4\text{-}6)$$

Another useful method to compute the transition matrix is by way of the inverse Laplace transform technique. The solution of the transition matrix may be written as (Hochstadt, 1975)

$$\Phi(t,o) = L^{-1}(sI - F) \qquad (4\text{-}7)$$

where

L^{-1} is the inverse Laplace transformation,

I is the identity matrix, and

s is the Laplace transform variant.

The transition matrix derived from equation (4-7) gives the analytical expression of the influences of each state error on the other

errors, thus it is called the analytical transition matrix here. The analytical transition matrix can also be obtained by the matrix exponent expansion method given by equation (4-5). To derive the expressions by expansion of the matrix exponential, one has to expand the series to many terms such that each element in the transition matrix is a sum of the corresponding elements in the matrices of the series. The analytical expressions may then be formed by inspecting the sums. This method is not used in this research because each sum has to be expanded to many terms before we can recognize what function it represents if it is recognizable at all.

The functions in the analytical transition matrix are useful in the study of the behaviour of the state errors over a given time interval, but the derivations of these functions are very lengthy and difficult. In this case, the inverse Laplace transform method is applicable but it involves the analytical inversion of a large matrix (at least 7×7), and it has to be repeated whenever there is a change in elements of the dynamics matrix. The analytical solution to the dynamics matrix given in Figure 3-1 is derived in the following sections. It will be used for the error propagation and analysis of the growth of the basic state errors in an LLISS over a time interval short enough to assume the dynamics matrix as constant. The derivation consists of two parts: the inversion of the matrix $(sI - F)$ and the solution by the inverse Laplace transform.

4.1 Inversion by Partitioning Method

The inversion of the matrix (sI - F) in equation (4-7) can be accomplished by the partitioning method described by Faddeev and Faddeeva (1963). The method inverts a matrix in the following way. Given a matrix

$$J = (sI - F) \quad , \tag{4-8}$$

partitioned into

$$J = \begin{bmatrix} \overbrace{A_1}^{A_2} & B_1 & B_2 \\ C_1 & D_1 & \\ C_2 & & D_2 \end{bmatrix} \quad , \tag{4-9}$$

the inverse of J can then be written as

$$J^{-1} = \begin{bmatrix} \overbrace{O_1}^{O_2} & L_1 & L_2 \\ M_1 & N_1 & \\ M_2 & & N_2 \end{bmatrix} \quad , \tag{4-10}$$

where

$$N_i = (D_i - C_i A_i^{-1} B_i)^{-1} \quad , \tag{4-11}$$

$$L_i = -A_i^{-1} B_i N_i \quad , \tag{4-12}$$

$$M_i = -N_i C_i A_i^{-1} \quad , \tag{4-13}$$

and

$$O_i = A_i^{-1} + A_i^{-1} B_i N_i C_i A_i^{-1} \quad . \tag{4-14}$$

In this way, the matrix J can be inverted, analytically, part by part. The inversion may begin with 2×2 sub-matrix in the upper left-hand corner and expands one row and one column at a time using the recursive equations (4-11) to (4-14) until the entire matrix is inverted. In this case, the dynamics matrix of the basic state errors is a 9×9 matrix, and the inversion is done in two steps. First, the top left 7×7 sub-matrix pertaining to the errors in the horizontal channels is inverted. A similar inverted matrix is given in Wong and Schwarz (1979). Second, the remaining parts of the J-matrix are added and inverted together with the first sub-matrix. If the dynamics matrix is extended to include other systematic errors, the expanded J-matrix can be inverted the same way using the inverted 9×9 basic matrix as the starting sub-matrix.

4.2 Inverse Laplace Transform Technique

Once the J-matrix has been inverted, the analytical expression for every element in the transition matrix may be obtained using the inverse Laplace transform technique. Sometimes, taking these inverse transforms is a very lengthy process. Often, the convolution theorem (Sokolaikoff and Redheffer, 1966)

$$L^{-1}(f_1(s),\ f_2(s)) = \int_0^t F_1(t-\tau)\ F_2(\tau)\ d\tau \qquad (4\text{-}15)$$

has to be applied to simplify the derivations. The elements in J^{-1} are mostly high degree polynomials of s. They have to be reduced to the products of two or more lower degree polynomials whose inverse

Laplace transform F_i can be found in tables, (e.g. McCollum and Brown, 1965). Integrating the analytical expressions on the right hand side of equation (4-15) may also be difficult. Fortunately, the lengthy integrals in these expressions can usually be found in mathematical handbooks, e.g. Spiegel (1968). Examples of such integrated expressions are given in Wong and Schwarz (1979).

4.3 Additional State Errors

Systematic errors in the instruments, if not corrected, can be included in the state errors. The transition matrix for the extended state vector is a derivative of the basic matrix mentioned in the previous section. For errors such as drift rates and biases, the additional rows and columns of the extended dynamics matrix contain only zeros, except for the rows associated with the basic errors they influence. In this case, the lower right sub-matrix of J pertaining to the additional errors consists of s whose inverse Laplace transform is 1. The M_i part of J^{-1} is null because the basic state errors have no influence on the instrument errors.

As an example, the dynamics and transition matrix of an extended state vector that contains a drift rate of the vertical axis is shown here. The dynamics matrix has the form

$$F_{10\times 10} = \left[\begin{array}{c|c} F_{9\times 9} \\ \text{(from Figure 3-1)} & \begin{matrix}0\\0\\1\\0\\\vdots\end{matrix} \\ \hline 0\ \ 0\ \ 0\ \ \ldots\ldots & 0 \end{array}\right] . \qquad (4\text{-}16)$$

and its J matrix is

$$J_{10\times 10} = \left[\begin{array}{c|c} J_{9\times 9} & \begin{matrix}0\\0\\-1\\\vdots\end{matrix} \\ \hline 0\ 0\ 0\ \ldots. & s \end{array}\right]$$

Since the C_2 part of this matrix (see equation (4-9)) contains only zeros, the N_2 and L_2 of the inverted J can be written as

$$N_2 = \frac{1}{s} \quad , \tag{4-18}$$

and

$$L_2 = -J^{-1}_{9\times 9}\begin{bmatrix}0\\0\\1/s\\0\\\vdots\\0\end{bmatrix} \quad . \tag{4-19}$$

The M_2 and O_2 of $J^{-1}_{10\times 10}$ can be reduced to zero and $J^{-1}_{9\times 9}$ respectively because C_2 is zero. By combining the inverse Laplace transforms of equations (4-18) and (4-19) and the 9×9 Φ-matrix mentioned in the previous section, the analytical transition matrix of the 10×10 dynamics matrix can be obtained as

$$\Phi_{10\times 10} = \left[\begin{array}{c|c} \Phi_{9\times 9} & \begin{matrix}\int_o^t \Phi(1,3)d\tau\\ \int_o^t \Phi(2,3)d\tau\\ \vdots\end{matrix} \\ \hline 0\ 0\ 0\ \ldots & 1.0 \end{array}\right] \quad .$$

The analytical expressions for this 10×10 transition matrix are listed in Appendix C.

Chapter 5

KALMAN FILTERING AND SMOOTHING

A properly designed transition matrix can predict the changes of the state errors over a given time interval but it does not produce any estimate on the size of the random noise accumulated in the system. The initial conditions x(o) of the linear system described by equation (4-1) are usually unknown. The size of the initial state errors of an LLISS can only be described statistically. They change from one alignment of the system to the next and therefore they cannot be predicted before the survey. They can be estimated, however, when external control measurements become available. Any external measurement that can be expressed as a linear function of one or more of the state errors is usable. These measurements also help us to check the growth of uncertainties in the predicted state errors. For a land vehicle mode LLISS, the simplest control measurements available are the velocity errors detected in the system at vehicle stops. The velocity outputs given by the system when it is not moving represent the velocity state errors of the LLISS.

There are different methods available for utilizing the velocity observations as a means to estimate the state errors. The method used here is Kalman filtering. An optimal Kalman filter to estimate the position coordinates and their variance-covariances for the measurements given by the FILS is developed in this chapter.

5.1 Filtering Equations

The derivation of the optimal Kalman filtering equations is well documented, e.g. Gelb (1974), therefore only a summary of formulae and the implementation of the equations in inertial surveying are discussed here. Given that the solution of a set of linear differential equations that describe the dynamics of an LLISS is of the form

$$x(t) = \Phi(t,o)\ x(o) \quad , \tag{4-4}$$

and the control measurements obtained at epoch k are

$$z_k = H_k x_k + y_k \quad , \tag{5-1}$$

where

H_k is the design matrix $\frac{\partial z}{\partial x}$

and y_k is the measurement noise.

The state vector and its variance matrix can be updated, i.e. improved in terms of accuracy, by the equations:

$$x(-) = \Phi_{k,k-1}\ x_{k-1}(-) \ ; \tag{5-2}$$

$$P_k(-) = \Phi_{k,k-1}\ P_{k-1}(-)\ \Phi^T_{k,k-1} + Q_k \ ; \tag{5-3}$$

$$x(+) = x_k(-) - K_k(H_k x_k(-) - z_k) \ ; \tag{5-4}$$

$$P_k(+) = (I - K_k H_k)\ P_k(-) \ ; \tag{5-5}$$

$$K_k = P_k(-)\ H_k^T(H_k P_k(-)\ H_k^T + R_k)^{-1} ; \tag{5-6}$$

$$Q_k = \int_o^{t_k - t_{k-1}} \Phi_{k,k-1}\ \bar{Q}\ \Phi^T_{k,k-1} \ ; \tag{5-7}$$

where

K_k is the Kalman gain matrix,

P_k is the variance matrix of the state vector,

R_k is the variance matrix of the control measurements,

$\bar{Q}$ is the spectral density matrix of the noise in the system,

(-) symbolizes the quantities before update, and

(+) symbolizes the quantities after update.

With this set of equations, all the information gathered since the beginning of the survey is used to estimate the state vector at epoch k. The function of the transition matrix is the propagation of the information to the epoch in question for the measurement update. There are questions about the transition matrix and the update equations which must be answered before these quantities can be implemented as linear estimation tools. The following information is needed before implementation: the size of the state vector; the characteristics of the design matrix; the initial variance matrix P(o) and the changes in the dynamics matrix in between updates.

5.1.1 The State Vector

Many of the instrument errors in the FILS are internally corrected by the system. These errors are the three drift rates, the scale errors in the horizontal channels and the non-orthogonality of the accelerometers. They are regularly determined from survey data obtained from calibration runs over accurately established base lines. The errors are fed into the system prior to an inertial survey so

that the effects of the time invariant errors can be removed from the data before they are recorded. The calibration errors are usually good approximations to the actual errors because the remaining errors are small compared to both basic errors and the white noise in the system. Thus, taking the remaining errors in the state vector usually does not improve the accuracy of the estimates but it can increase the computation time considerably. The results of the calibration runs show that the size of the drift rate of the vertical axis δd_U is comparatively large relative to other drift rates; therefore its remaining error is expected to be larger. Based on all the considerations mentioned, the state vector used in the reported research is

$$x = \{ \varepsilon_E, \varepsilon_N, \varepsilon_U, \delta\phi, \delta\lambda, \delta\dot{\phi}, \delta\dot{\lambda}, \delta h, \delta\dot{h}, \delta d_U \}^T \qquad (5\text{-}8)$$

The gravity disturbances are not modelled here because the survey data used for testing the filter were obtained from a base line on gentle terrain where the sizes of the deflections of the vertical and the gravity anomaly are small and they do not change drastically with distance. The gravity anomaly at the initial point is normally observed during the alignment and removed from the specific force sensed by the system along the survey traverse.

5.1.2 Initial Weighting

The sizes of the initial errors are dependent on how accurately the system is aligned at the starting point of the survey. With a properly calibrated system these errors are random from one survey to

the next. Statistically, the mean value of the initial state vector between surveys is

$$E[x(o)] = 0 \qquad (5\text{-}9)$$

with variance matrix

$$P(o) = E[x(o)\ x(o)^T] \quad . \qquad (5\text{-}10)$$

The variances in P(o) are normally determined from a priori information about the accuracy of the alignment, of the control coordinates and of the system itself. Data from calibration runs can give a good indication on the accuracy of the alignment. The attitude errors are usually treated as uncorrelated quantities because the alignments of the three platform axes may be considered as independent. The velocities in the system are always equal to zero at t = 0. Obviously they are not correlated with other state errors. The variances of the position errors are dependent only on the accuracy of the input coordinates. The constant remaining drift rate can be as large as the input drift rate computed in the calibration adjustment (see Deren and Hagglund, 1981 for details on the adjustment). Based on the velocity data and considerations mentioned above, the initial weighting for the Kalman filter developed in this research is tabulated in Table 5-1. The error ε_U has a much larger 1σ value because gyrocompassing is less accurate than levelling. The 10 m and the 1 cm/s deviations for the input coordinates and velocities may be too pessimistic but, in post-mission filtering,control coordinates and velocities and their variances can be introduced into the estimate through control measurement updates at the starting point.

state errors	1σ
ε_E	5 arc sec
ε_N	5 arc sec
ε_U	100 arc sec
$\delta\phi$	10 m
$\delta\lambda$	10 m
$\delta\dot{\phi}$	0.01 m/sec
$\delta\dot{\lambda}$	0.01 m/sec
δh	10 m
$\delta\dot{h}$	0.01 m/sec
δd_U	0.5 arc sec/sec

Table 5-1 : Standard Deviation of the Initial State Vector

Another important weighting process is the choice of the spectral density for the matrix $\bar{Q}$. The matrix is a diagonal matrix whose non-zero elements represent the stochastic expectations of the square of the noises accumulated in the corresponding state errors per unit of time. Their sizes are dependent on the average magnitudes of the random uncertainties in the sensors which cannot be systematically predicted by the transition matrix. The values of these elements can be obtained from the results of calibration tests or experiments in the laboratory. Due to the lack of this kind of information, the values of the non-zero elements selected for this research are based on values implemented in other local level systems.

They are then compared with the actual errors fed back from the testing. The estimated noise densities used here are $2.25 \cdot 10^{-6} m^2 \cdot sec^{-3}$ for velocity noise and 0.003 arc $sec^2 \cdot sec^{-1}$ for attitude error noise. The results of the comparison of these numbers with actual errors after filtering will be discussed in the next chapter.

5.1.3 Error Propagation

The analytical expressions of the transition matrix are derived under the assumption that the dynamics of the system is constant. To satisfy this condition, the error propagation interval Δt has to be chosen small enough so that changes in velocity and position of the vehicle are negligible compared to the quantities themselves. Since the vehicle has to move from point to point, it is impossible to maintain the constant dynamics condition between velocity updates. The total transition matrix between the update epochs k-1 and k has to be computed from the equation

$$\Phi(t_k, t_{k-1}) = \prod_{i=0}^{n-1} \Phi(t_i + \Delta t, t_i) \qquad (5\text{-}11)$$

where

$$n = \frac{t_k - t_{k-1}}{\Delta t} \qquad (5\text{-}12)$$

and

$$t_i = t_{i-1} + (i + 0.5)\,\Delta t \ . \qquad (5\text{-}13)$$

The value of Δt does not have to be constant. The FILS dumps velocity data at different time intervals during different stages of

the survey. The system records velocity data at approximately every 0.6 seconds during the update period and increases the interval to 10 seconds while travelling. Thus, equation (5-11) can still be applied but the value of n is the number of velocity data records available between updates.

The propagation of the noise variance matrix Q_k is described by equation (5-6). Again, it can be performed either numerically or analytically. The analytical approach was chosen in this case because it is less time consuming. The derivation of the analytical expression of the variances and covariances in Q_k is a lengthy process. Fortunately, many of the correlations in the matrix are very weak for a small time interval. Their magnitudes are of the order of 10^{-2} for $\Delta t \leq 10$ seconds, therefore they can be neglected. The expressions for other variances and covariances, for a small time interval, are given in Appendix D.

5.1.4 Control Measurement Updates

There are three types of control information which can be used to update the error state of a land vehicle mode LLISS: the velocity errors, the position errors, and the gravity disturbances if they are modelled in the state vector. In most surveying applications, the gravity information of the area of interest is not available. Users normally have to rely on the velocity and coordinate updates to improve the accuracies of the LLISS estimates. Since gravity anomalies and deflections of vertical are not part of the state vector in this research, only the velocity and coordinate updates are discussed in this section.

5.1.5 Design Matrix

The optimal Kalman filter described in section 5.1 accepts any type of measurements to update its error states provided the measurements can be expressed in the explicit form given by equation (5-1). The land vehicle mode LLISS stops regularly to gather velocity information to update its state vector. The process is commonly known as a zero velocity update (ZUPT). The 3 velocities ($\dot{\phi}$, $\dot{\lambda}$, $\dot{h}$) given by the system at a stop are the velocity errors accumulated in the course of the survey. The design matrix that links them to the state errors has the simple form

$$H = \begin{bmatrix} 0 & 0 & 0 & 0 & 0 & 1 & 0 & 0 & 0 & 0 \\ 0 & 0 & 0 & 0 & 0 & 0 & 1 & 0 & 0 & 0 \\ 0 & 0 & 0 & 0 & 0 & 0 & 0 & 0 & 1 & 0 \end{bmatrix} . \qquad (5\text{-}14)$$

Coordinate information can also be used as control measurements during zero velocity update. In that case, the vector z_k contains the differences between the control coordinates and the uncorrected coordinates given by the LLISS. The design matrix is just as simple as equation (5-14) with the unit values in position H(1,4), H(2,5) and H(3,8).

5.1.6 Velocity and Coordinate Updates

In general, the zero velocity update period of an LLISS is between 25 and 30 seconds. The FILS dumps up to 30 velocity readings in this period. Since the period is so short, the 3 velocity measurements have very little effect on each other, and the correlations

between them are practically zero. Based on this assumption, the update process may be carried out with one velocity measurement at a time. The computations are simpler in this case because the inversion in equation (5-6) is reduced to a division. As shown in Appendix E, the gain matrix may be computed by

$$K(i, 1) = P(i, j) / (P(j, j) + R) \ , \qquad (5\text{-}15)$$

where $P(j, j)$ is the variance of the velocity state error and R becomes the variance of the observed velocity. The same approach is also applicable for coordinate updates if the control coordinates are treated as uncorrelated quantities.

The control measurement update is usually done at the end of the update period. A simple adjustment program has been developed to compute the velocities at the end of the update period using all the 30 to 32 velocity outputs. The program assumes that the velocity errors are observed independently and the acceleration errors in the update period are constant. The velocities at the end of the update can be computed by the equation

$$\tilde{v}_j = \frac{\sum_{i=1}^{m} \Delta t_i^2 \cdot \sum_{i=1}^{m} \hat{v}_i - \sum_{i=1}^{m} \Delta t_i \cdot \sum_{i=1}^{m} \Delta t_i \, \hat{v}_i}{m \sum_{i=1}^{m} \Delta t_i^2 - \sum_{i=1}^{m} \Delta t_i \cdot \sum_{i=1}^{m} \Delta t_i} \ . \qquad (5\text{-}16)$$

Their variance is

$$\sigma\tilde{v}_j^2 = \frac{\sigma\hat{v}_j^2 \sum_{i=1}^{m} \Delta t_i^2}{m \sum_{i=1}^{m} \Delta t_i^2 - \sum_{i=1}^{m} \Delta t \cdot \sum_{i=1}^{m} \Delta t} \quad , \qquad (5\text{-}17)$$

where

m is the number of velocity measurements and

$\Delta t = t_i - t_m$.

The quantity $\sigma\hat{v}_i^2$ is the variance of a single velocity measurement which can be estimated from the a posteriori variance factor of the adjustment.

5.2 Cross-Variance Equation

The Kalman filter equations given in section 5.1 yield only the variance-covariance between coordinates of the same point. Since the vector $x_k(-)$ is directly related to the vector $x_{k-1}(+)$, it is not difficult to see that the coordinates between two neighbouring points on the same traverse are strongly correlated. The equation for computing the cross-variances between any two points is given in Schwarz (1980b):

$$P_{k,k+j}(+) = P_k(+) \prod_{i=1}^{j} \Phi^T_{k+i,k+i-1} (I - K_{k+i} H_{k+i})^T \quad . \qquad (5\text{-}18)$$

This equation is used to study the effects of velocity and coordinate updates on the correlations between coordinates of different points in an inertial survey.

5.3 Smoothing Equations

The derivations of the optimal smoothing equations are well documented in Gelb (1974). Basically, the smoothing equations take all the information collected after the epoch in question to improve the estimates given by the filter. The original smoothing equations involve the inversion of a matrix of the size of the matrix P. They can become very time consuming and unstable when the size of the state vector is very large. A set of recursive optimal smoothing equations that avoids such inversions has been given by Bierman (1973). The smoother developed in this research uses this set of equations to back-smooth the results of the filtering. The equations are

$$x_k^s(+) = x_k(+) - P_k(+)\, \chi_k(+) \quad , \tag{5-19}$$

$$P_k^s(+) = P_k(+) - P_k(+)\, X_k(+)\, P_k(+) \quad , \tag{5-20}$$

$$\chi_k(+) = \Phi_{k+1,k}^T\, \chi_{k+1}(-) \quad , \tag{5-21}$$

$$X_k(+) = \Phi_{k+1,k}^T\, X_{k+1}(-)\, \Phi_{k+1,k} \quad , \tag{5-22}$$

$$\chi_k(-) = (I - K_k H_k)^T\, \chi_k(+) + H_k^T\, D_k^{-1} (H_k x_k(-) - z_k) \quad , \tag{5-23}$$

$$X_k(-) = (I - K_k H_k)^T\, X_k(+)\, (I - K_k H_k) + H_k^T\, D_k^{-1}\, H_k \quad , \tag{5-24}$$

and $$D_k = (H_k\, P_k(-)\, H_k^T + R_k) \quad , \tag{5-25}$$

where the superscript s symbolizes quantities after smoothing. The smoothing starts at the end of the inertial survey mission by initializing

$$\chi_e(-) = H_e^T\, D_e^{-1}\, (H_e\, x_e(-) - z_e) \tag{5-26}$$

and $$X_e(-) = H_e^T\, D_e^{-1}\, H_e \tag{5-27}$$

where e is the last epoch of measurement update. The data needed for smoothing are the state vectors and their variance matrices before and after updates, the control measurements and their variances, the type of control measurements (velocity or coordinate), and the total transition matrices between updates.

Chapter 6

TESTING AND RESULTS

Three Fortran computer programs were written for the implementation of the Kalman filter, the cross-variance equations and the optimal smoother developed in this research. Data collected by different FILS-systems over a base line established by Sheltech Canada near Calgary were used to test the Kalman filter-smoother. The accuracies of the control coordinates ($1\sigma < 1$ m) were considered to be superior to the measurement accuracy of the FILS. Results of the testing are presented and analyzed in this chapter.

6.1 Descriptions of the Software

The Kalman filtering program developed here was designed for post-mission use. It filters the raw velocity and coordinate data gathered by the FILS and computes the coordinates of the stations on a survey line. The package consists of a main program called MAIN and 11 sub-programs. The functions of the main program are to

(i) read the control information and weights;

(ii) read the FILS data;

(iii) propagate the state vector and its variance matrix;

(iv) update the state vector and its variance matrix; and

(v) store the data needed for optimal smoothing.

The 8 sub-programs listed below were written to support the main program.

(i) UNIT converts the state vector and its variance matrix into proper units (e.g. radian to arcsec) for different computation and storage purposes.

(ii) UPDATE updates the state vector and its variance matrix with one control measurement at a time.

(iii) TMFLT generates the transition matrix with the analytical expressions derived in this research.

(iv) XYZNE was supplied by Sheltech Canada for computing position differences between the instrument origin and the protractor on the vehicle in the north and east directions.

(v) OFFST, also supplied by Sheltech Canada, computes the offset of the survey point from the protractor with the distance, horizontal angle and height difference measured during zero velocity update.

(vi) MOUTP reads and writes filtered data from or to storage files in special formats so that they can be easily read by the optimal smoothing program.

(vii) NORGRA computes the normal gravity at a given latitude and height.

(viii) RADIUS computes the distance to the centre of the earth with a given latitude and height.

The utility subroutine MOUTD prints the results of the filtering such as the vector x and the matrix P. The subroutine RTDMS converts radians to degrees, minutes and seconds. The function DMSTR converts degrees, minutes and seconds to radians. The linkage

between the main program and the sub-programs is shown in Figure 6-1.

After filtering, the order of the data file created by program MAIN must be reversed by a simple Fortran program called REARR before it can be used for computing the cross-variances or for optimal smoothing. The inversion requires a lot more storage space than the filtering program and it can only be done at the end of the filtering, therefore the program REARR was written as a separate utility program. The computation of the cross-variances and the optimal smoothing are performed by two separate main programs. Both programs can use the same data file mentioned above.

The program CROSS computes the cross-variance between a state vector element at any point of the survey with another state vector element at a different point of the survey.

The program SMOOTH, smooths the data after filtering with the recursive smoothing formulae given in chapter 5. The program back-smoothes the updated state vector three measurements at a time. In this way, the size of the data file generated by the filter is much smaller but the 3×3 inversion of the matrix D becomes unavoidable. INV is a simple utility subroutine written for inverting such a matrix.

The author's major consideration when writing these programs was the storage space requirement. The filtering package was designed to use up as little space as possible so that it can easily be modified for real-time application in a small on-board computer. The cross-variance computation and smoothing programs were written under the assumption that a more powerful computer is available in post-mission computation.

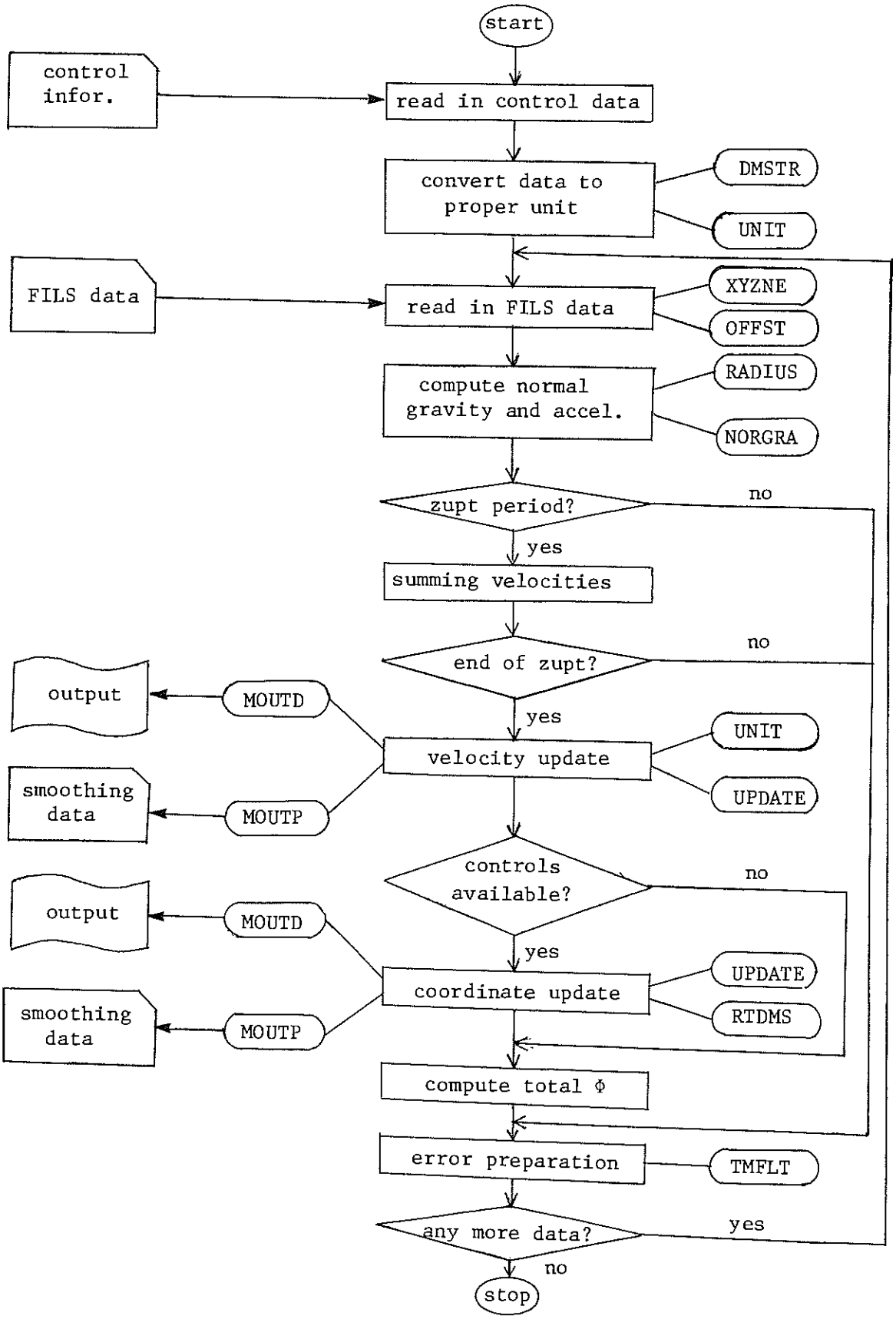

Figure 6-1 : Flow Chart of the Filtering Program

6.2 Tests

The test data used were collected with the FILS owned by Sheltech Canada. The surveys were part of their calibration programs which are carried out periodically to determine the instrument errors in the systems. Normally, several surveys are conducted over an L-shaped base line near Calgary. The error parameters (i.e. scale errors, drift rates and non-orthogonality) can be determined from an external adjustment with the velocity and coordinate data gathered in the first couple of runs. They are then fed back into the system at the beginning of the remaining surveys to correct for the effects of these instrument errors. The corrected velocity and coordinate data were used in this research because the transition matrix is derived under the assumption that instrument errors are corrected internally in the LLISS. Three such sets of calibration data were obtained from Sheltech Canada for the testing of the Kalman filter-smoother.

The base line is a 42 km L-shaped traverse which consists of 14 control points. The average height of the points is about 1 000 m and the maximum height difference between any two points is less than 90 m. The control coordinates were determined by conventional survey methods to second-order accuracy. Figure 6-2 shows the general configuration of the L-shaped base line.

6.3 Results

The data of the inertial surveys on the base line were filtered and smoothed in two control point modes:

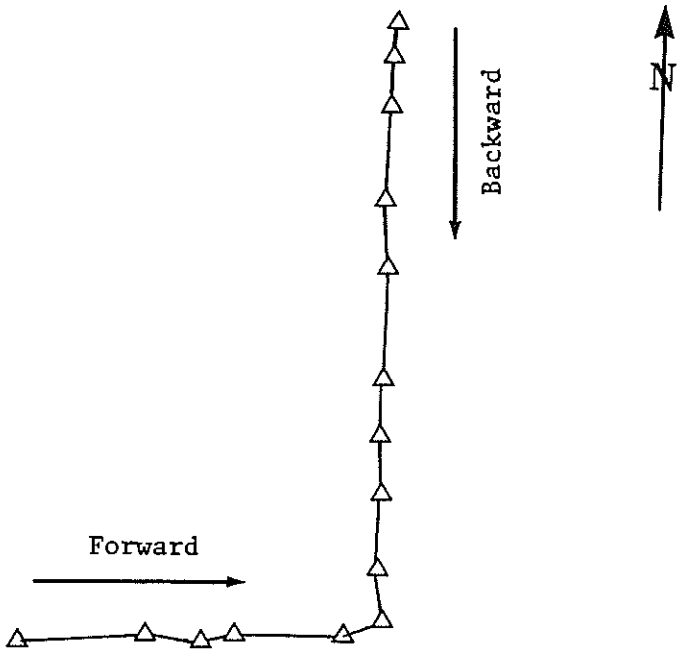

Figure 6-2 : Base Line

(i) control coordinate updates at both ends of the base line, i.e. three coordinate updates in one complete mission (forward and backward);

(ii) control coordinate updates at both ends and at the corner point of the L-shaped base line, i.e. five coordinate updates in one complete mission.

The surveys began at the west end of the base line. Each complete survey mission consists of a forward and backward run. The difference between the filtered or smoothed coordinates and the control coordinates not used in the coordinate updates were considered as the errors in the coordinates. The changes of these errors with respect to time or distance from the west end of the base line are presented in Figure 6-3 to Figure 6-20.

6.3.1 Two Control Points

Figures 6-3, 6-4 and 6-5 show the latitude, longitude and height errors in the filtered coordinates assuming that only the control points at the ends of the base line are known. The horizontal errors in these surveys are less than 10 m and the error curves are non-linear. The arrow heads indicate the epochs at which the FILS reached the corner point of the base line. Many of the curves bend at these epochs indicating that azimuth-dependent errors are present in the horizontal coordinates, which may either be due to the effects of the uncorrected residual scale errors or caused by the inaccuracy in the azimuth predicted by the Kalman filter. The height errors are less than 4 m and they grow linearly with time. These errors are smaller than the horizontal coordinate errors because the height differences between points are much smaller than their differences in latitude and longitude. Thus, scale factor errors are negligible. The variances of ϕ and λ given by the filter are quite compatible with the actual size of the horizontal coordinate errors but the height variances are, in many points, slightly pessimistic. The height variances can be reduced to a realistic size by choosing a small spectral variance density for vertical velocity, i.e. in element $\bar{Q}(9,9)$.

The errors in the smoothed coordinates are plotted in Figures 6-6, 6-7 and 6-8. After smoothing, the latitude errors are reduced to the metre range. The results of the back runs are, in general, better than the forward runs indicating that the coordinate update at the end of the forward runs improves the accuracies of the predicted

azimuths. The smoothed longitudes are less accurate than the latitudes and the accuracies of the backward runs are not much different from the forward runs. The signs of the horizontal coordinate errors, with the exception of the longitude in the first survey, change when the system turns around. Obviously, some azimuth or scale factor related errors were not completely removed by smoothing. The height errors, after smoothing, are down to sub-metre range but most of them are negative. The smoothed position variances are,in general, slightly pessimistic. More realistic variances can be obtained by reducing the elements $\bar{Q}(6,6)$ and $\bar{Q}(7,7)$ to $1.0 \cdot 10^{-6} m^2 \cdot s^{-3}$ and $\bar{Q}(9,9)$ to $0.49 \cdot 10^{-6} \cdot m^2 \cdot s^{-3}$. Table 6-1 shows the maximum coordinate variances before and after changing $\bar{Q}$.

max	original (m^2)		reduced (m^2)	
	filtered	smoothed	filtered	smoothed
σ_h^2	24.0	6.0	5.0	2.0
σ_ϕ^2 & σ_λ^2	37.0	8.0	25.0	3.0

Table 6-1 : Maximum Variances Before and After Changes in $\bar{Q}$ matrix (2 controls)

The weighted means of the smoothed forward and backward runs are shown in Figures 6-9, 6-10 and 6-11 as function of distance from the first point. The reciprocals of the variances were used as the

weights. The latitude and height errors are less than 1 m but mostly negative. In general, the accuracy of the longitudes is slightly worse than that of the other coordinates. The results indicate that the Kalman filter-smoother can yield sub-metre accuracy (1σ) in a 42 km, two control points, L-shaped traverse which takes two hours to survey, if a well calibrated FILS is available.

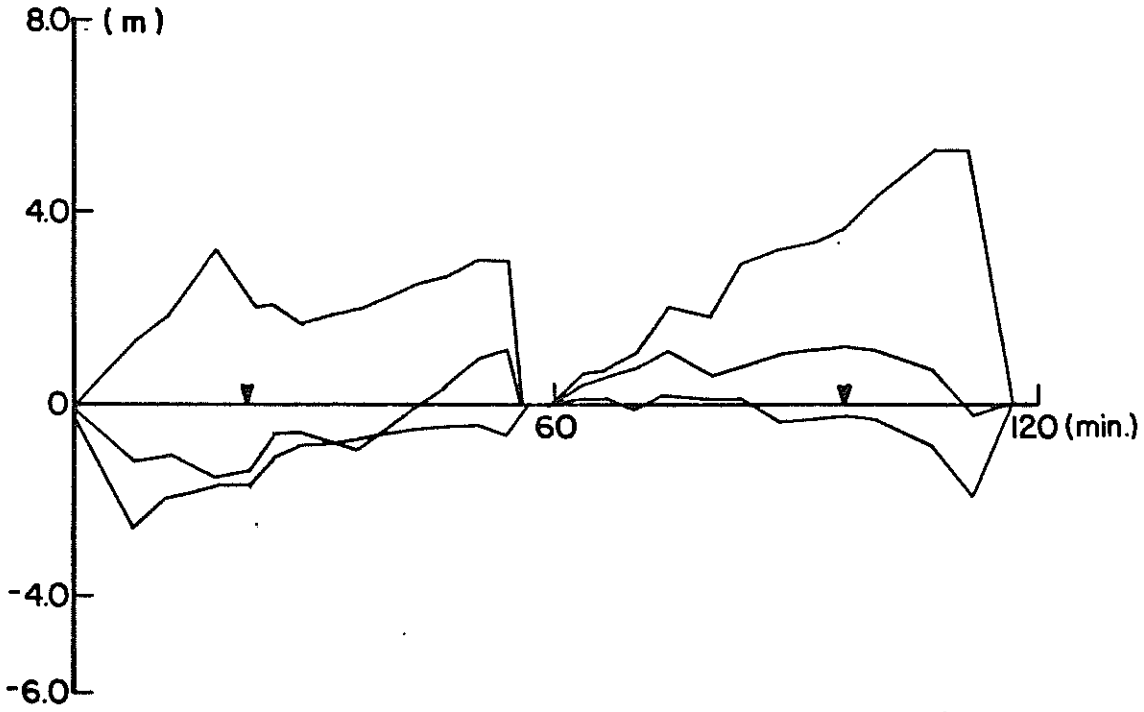

Figure 6-3 : Latitude Errors After Filtering (1^{st} case)

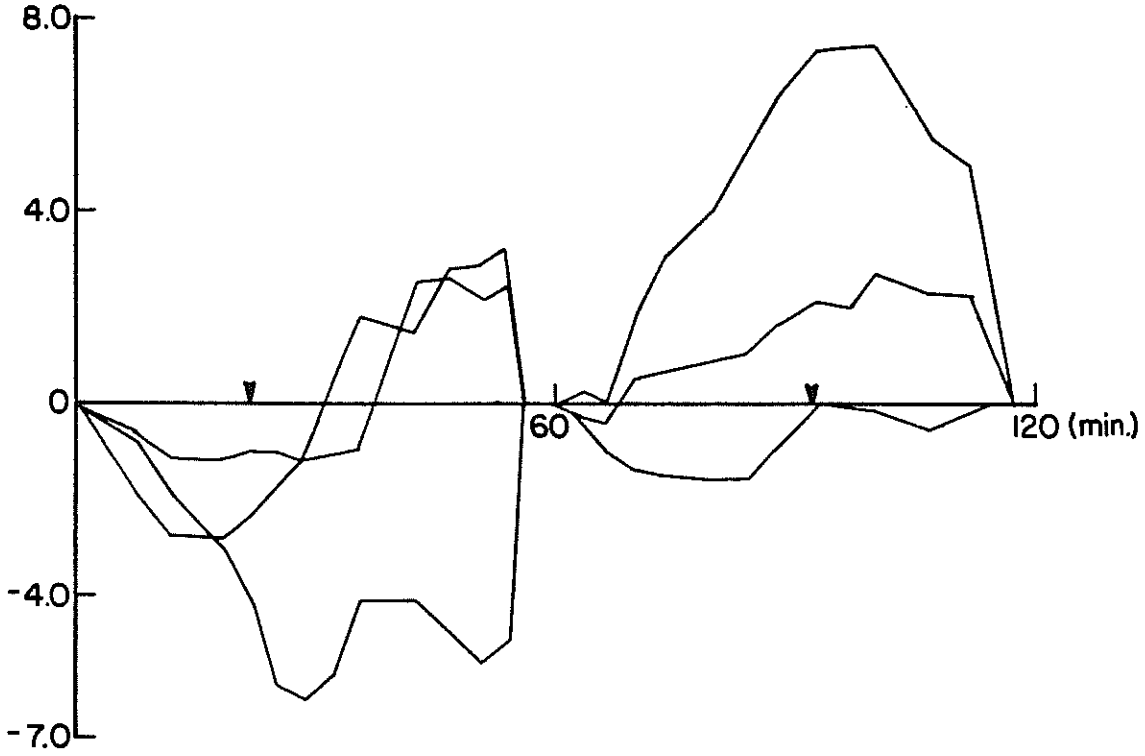

Figure 6-4 : Longitude Errors After Filtering (1st case)

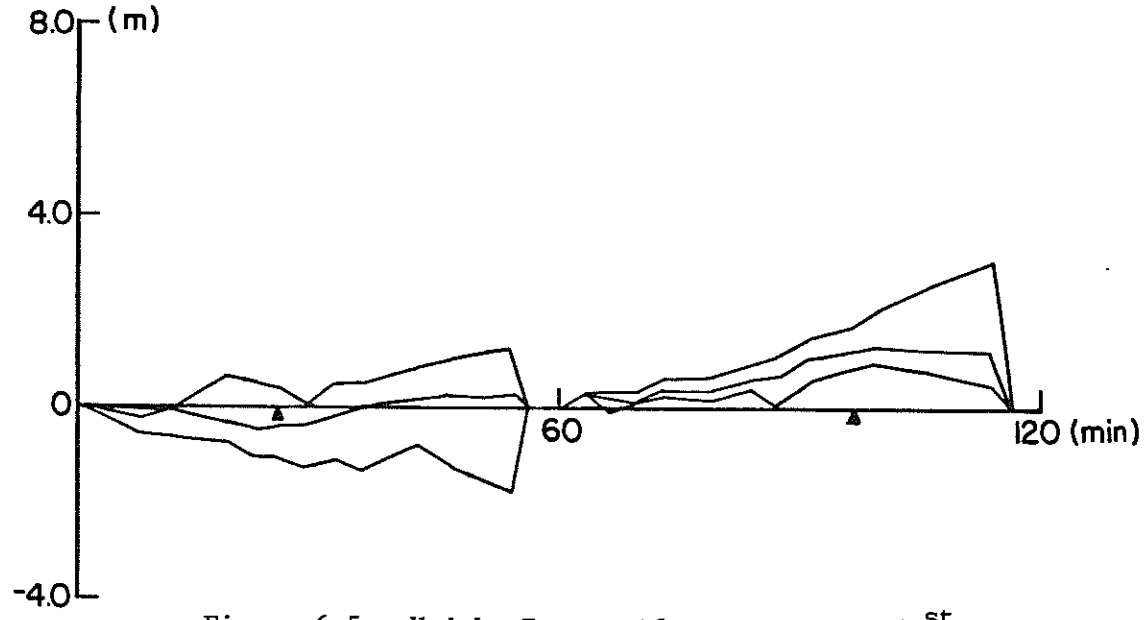

Figure 6-5 : Height Errors After Filtering (1st case)

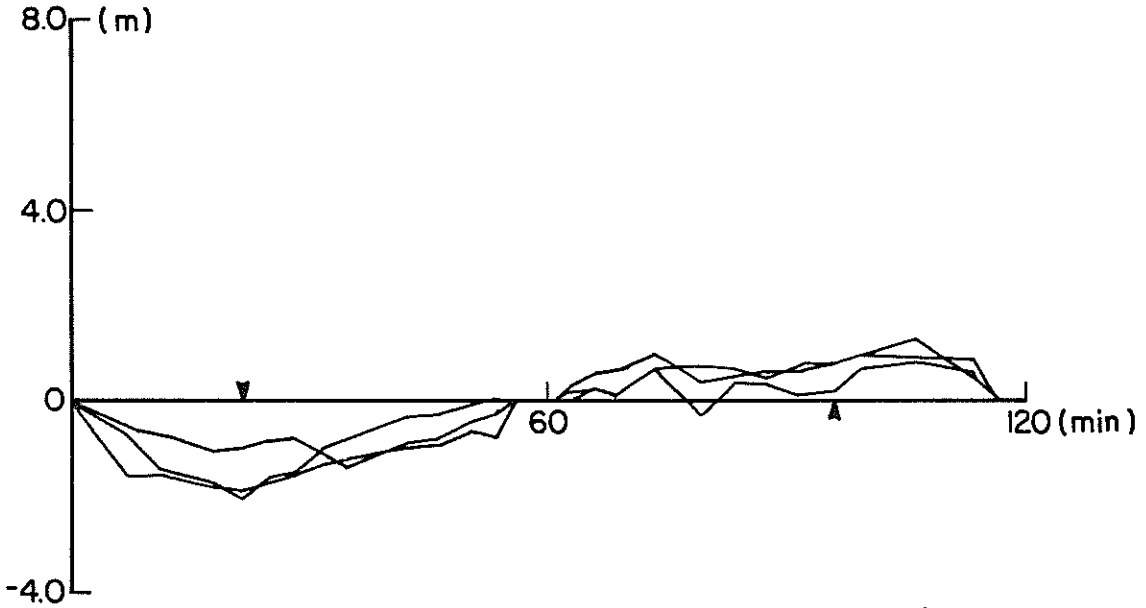

Figure 6-6 : Latitude Errors After Smoothing (1st case)

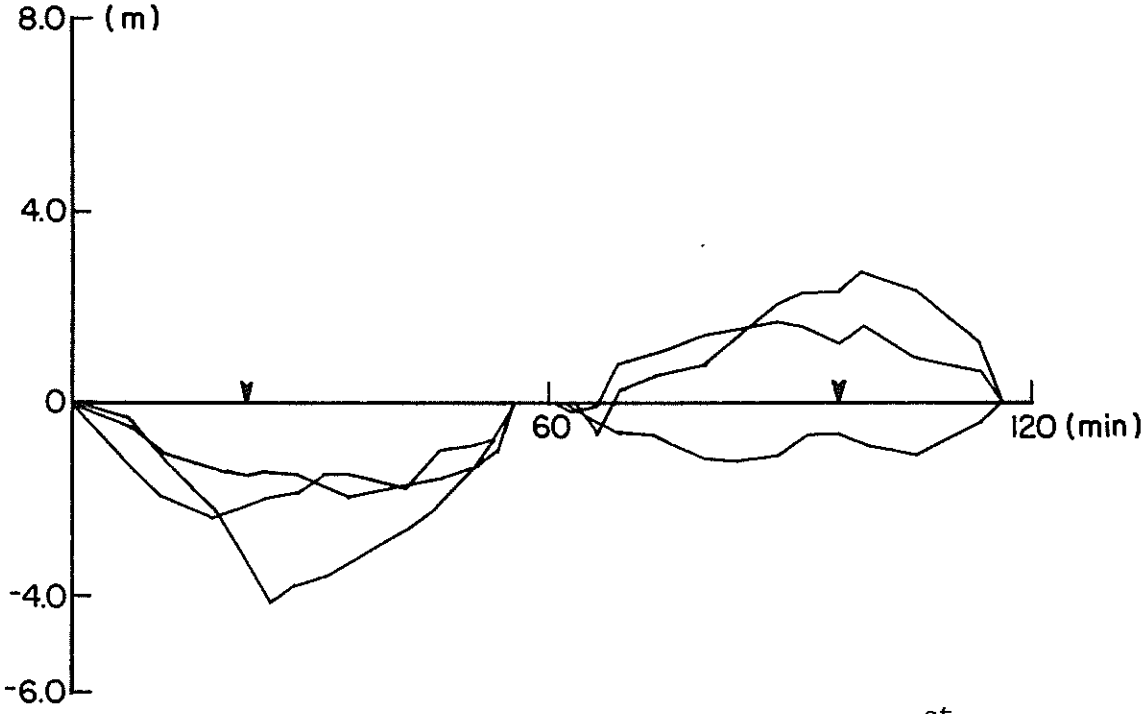

Figure 6-7 : Longitude Errors After Smoothing (1st case)

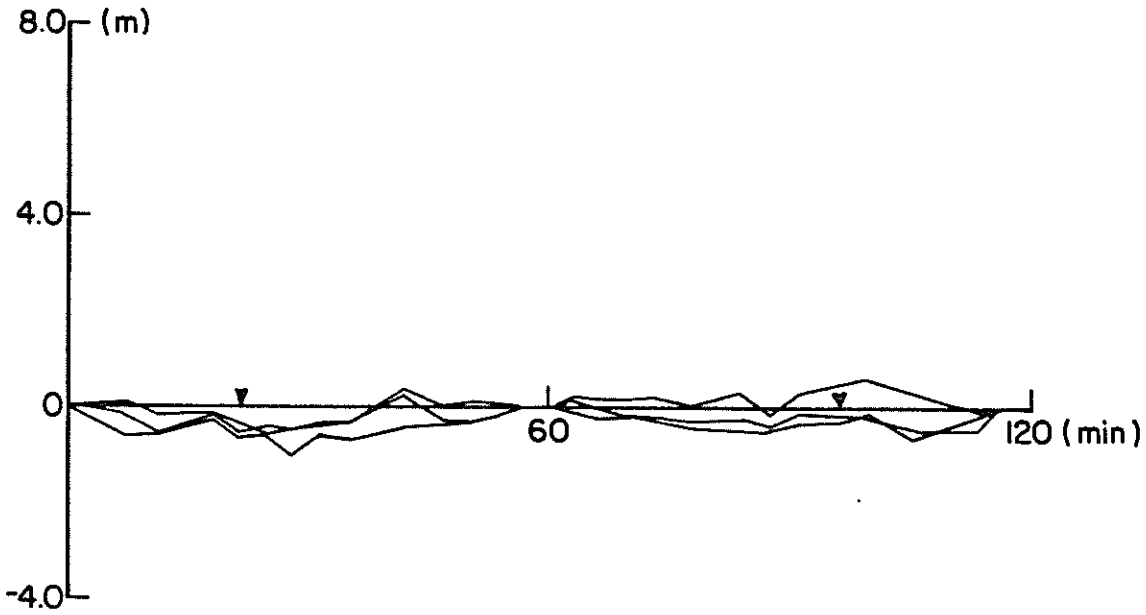

Figure 6-8 : Height Errors After Smoothing (1^{st} case)

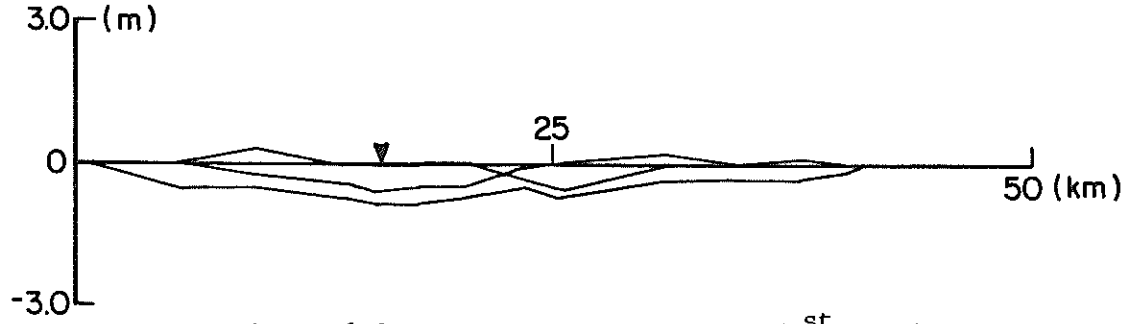

Figure 6-9 : Mean Latitude Errors (1st case)

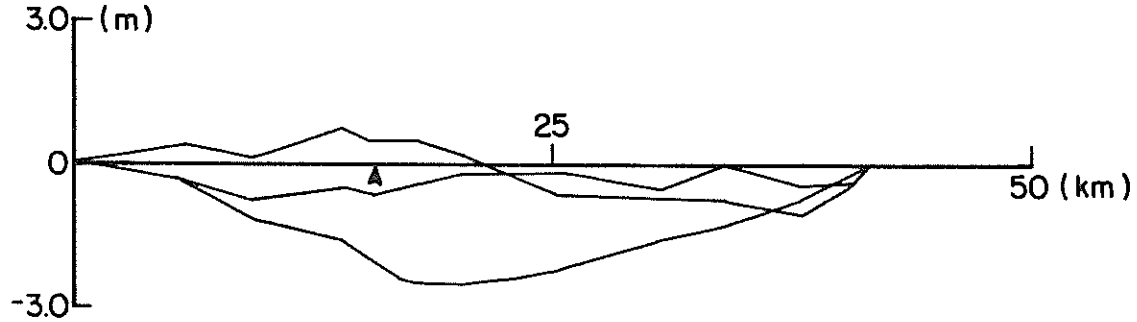

Figure 6-10 : Mean Longitude Errors (1st case)

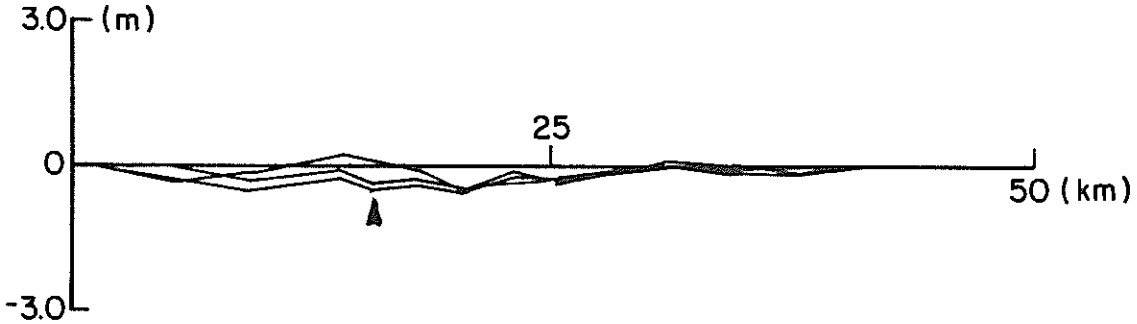

Figure 6-11 : Mean Height Errors (1st case)

6.3.2 Three Control Points

The three sets of data mentioned in the previous section were also filtered and smoothed by considering the point at the corner of the base line as known. As shown in Figures 6-12, 6-13 and 6-14, the error curves between control points are linear. The growth of the errors in the filtered coordinates is slightly smaller than in the case of two control points. The slopes of the latitude and longitude error curves become very gentle in the last leg. This shows that after a few coordinate updates the filter gains better control over the azimuth related errors. The additional coordinate control cannot change the time-dependent pattern of the height errors.

After smoothing, the latitude and height errors, as shown in Figures 6-15 and 6-17 are sub-metre in magnitude and they have become more random. The longitude errors in the backward runs are also less than 1 m but the errors in the forward runs are still in the metre range. The weighted mean errors in coordinates are all less than 1 m except three longitudes determined from the first set of data which are slightly above 1 m. The latitude and height errors have become completely random. As in the two control point mode, the variances given by the filter-smoother were too pessimistic, i.e. usually larger than the actual errors. Again, as shown in Table 6-2, they can be brought down to a more realistic level by reducing the spectral variance density of the velocities.

max.	original (m)		reduced (m)	
	filtered	smoothed	filtered	smoothed
σ_h^2	10.0	4.0	4.0	1.0
σ_ϕ^2 & σ_λ^2	25.0	4.0	8.0	2.0

Table 6-2 : Maximum Variances Before and After Changes in $\bar{Q}$ Matrix (3 controls)

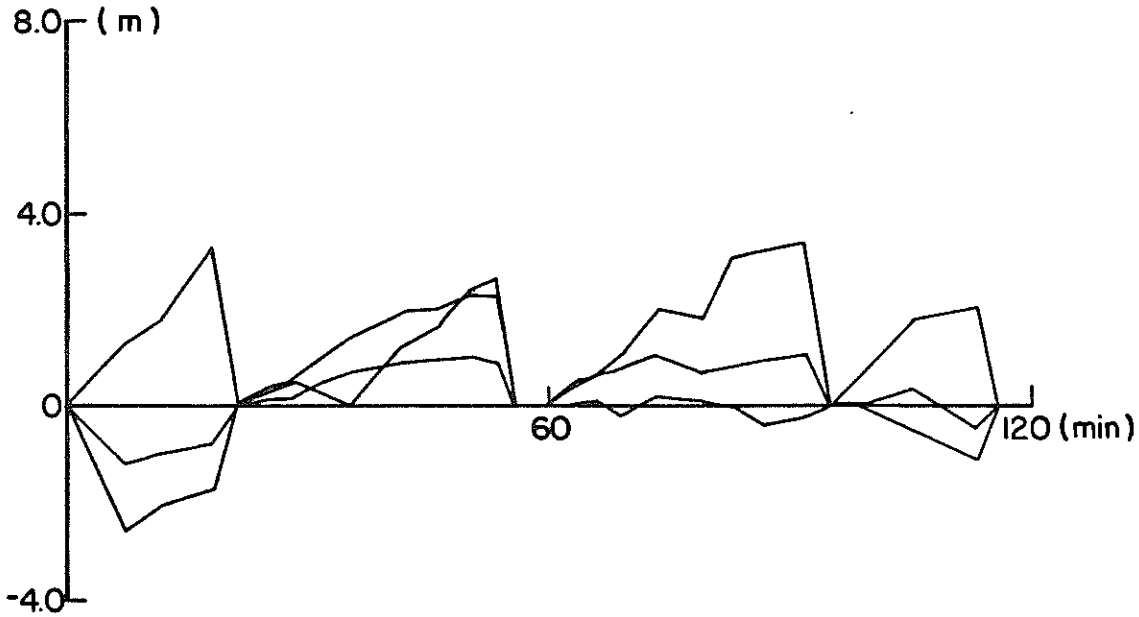

Figure 6-12 : Latitude Errors After Filtering (2^{nd} case)

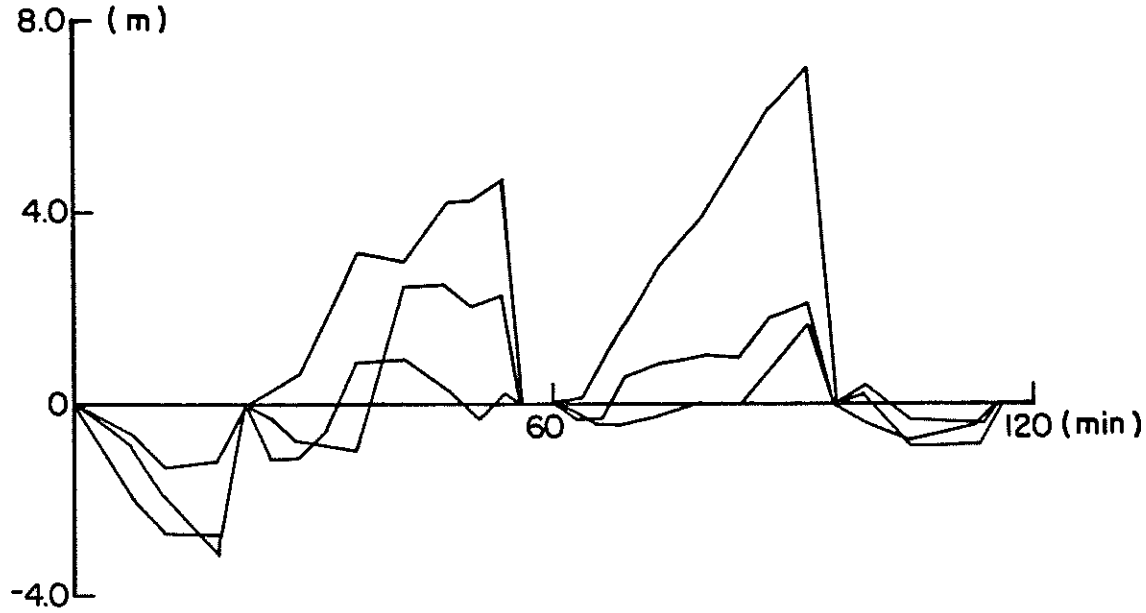

Figure 6-13 : Longitude Errors After Filtering (2^{nd} case)

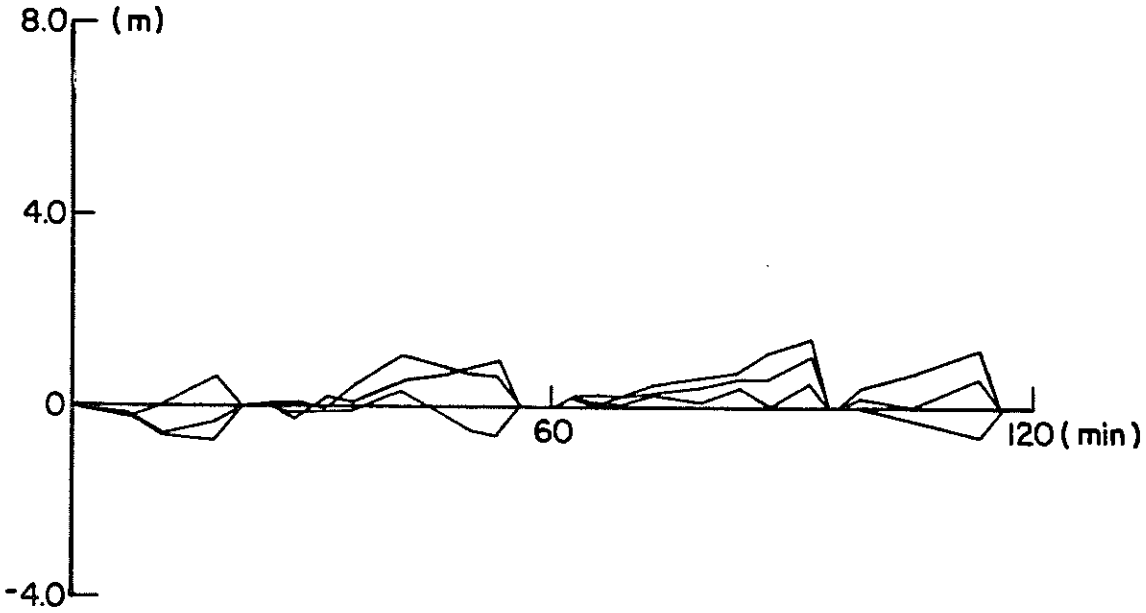

Figure 6-14 : Height Errors After Filtering (2^{nd} case)

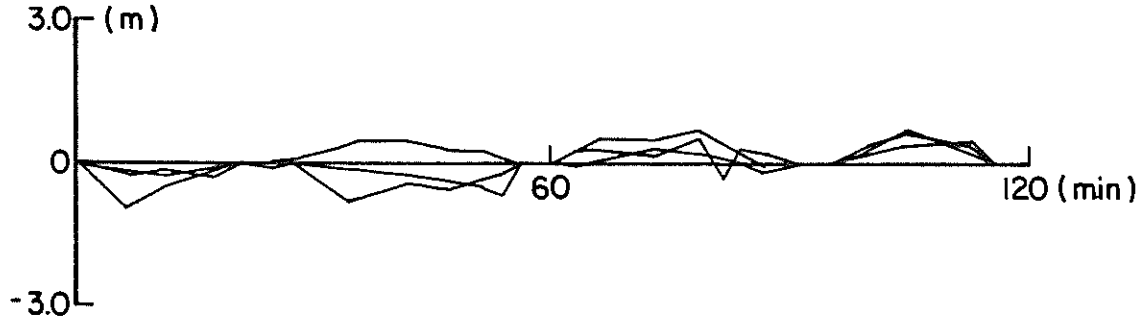

Figure 6-15 : Latitude Errors After Smoothing (2^{nd} case)

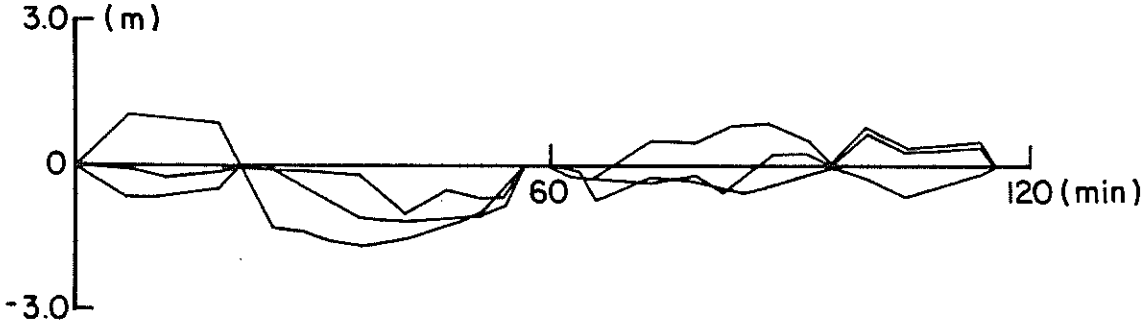

Figure 6-16 : Longitude Errors After Smoothing (2^{nd} case)

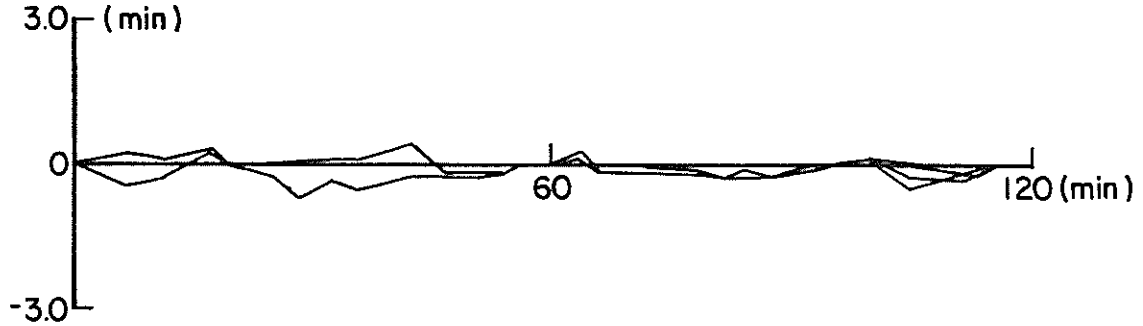

Figure 6-17 : Height Errors After Smoothing (2^{nd} case)

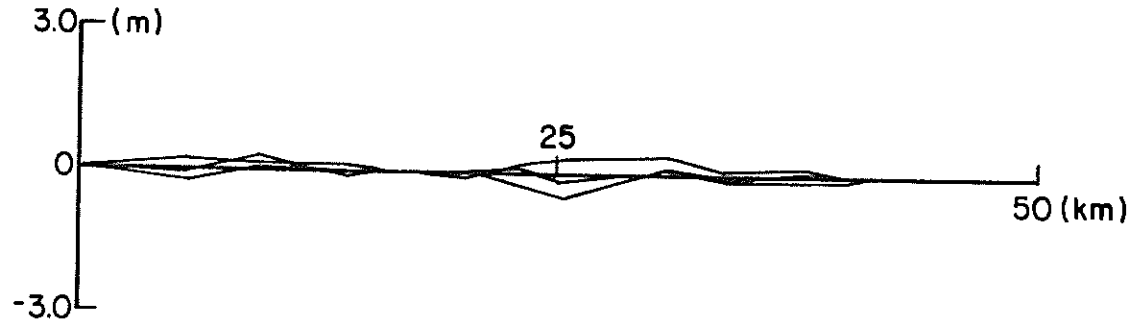

Figure 6-18 : Mean Latitude Errors (2^{nd} case)

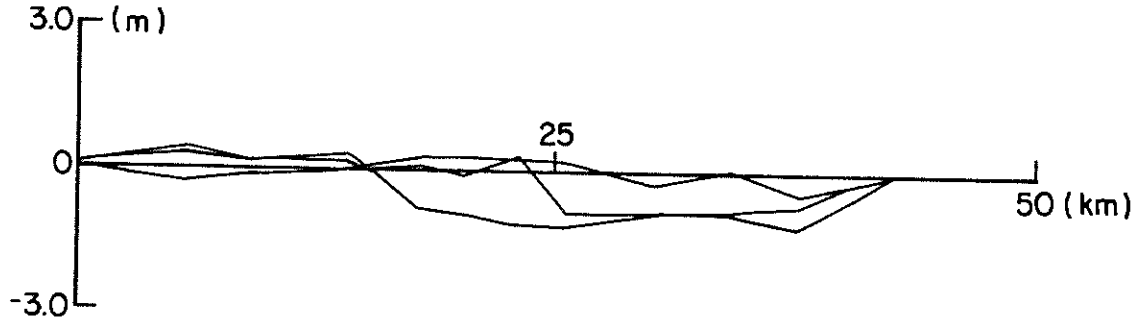

Figure 6-19 : Mean Longitude Errors (2^{nd} case)

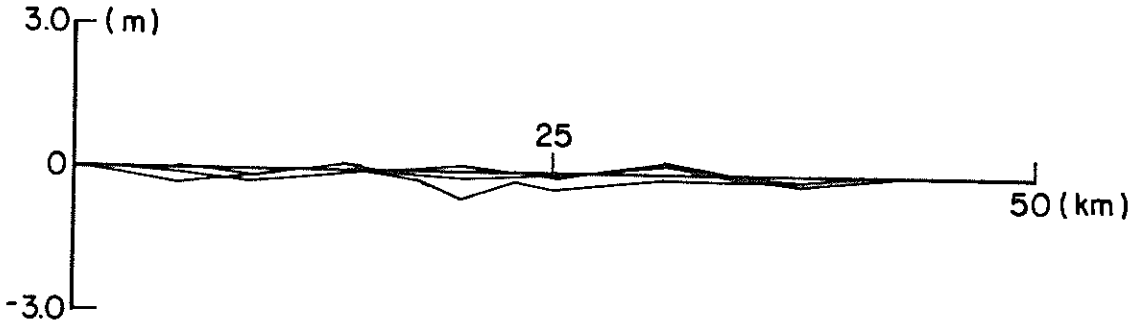

Figure 6-20 : Mean Height Errors (2^{nd} case)

6.3.3 Cross-Variances

The cross-variances between the state vectors of different updates were also computed from the filtered data. The results indicate that the position errors between two state vectors in between coordinate updates have a strong positive correlation. The correlation diminishes when the distance between the two points increases. Figure 6-21 is an example of the correlations between latitudes of a backward run.

*1.00									
0.03	1.00								
0.03	0.93	1.00							
0.02	0.84	0.90	1.00						
0.02	0.71	0.76	0.85	1.00					
0.01	0.54	0.58	0.65	0.77	1.00				
0.01	0.39	0.42	0.47	0.57	0.75	1.00			
0.00	0.03	0.03	0.03	0.04	0.06	0.08	*1.00		
0.00	0.00	0.00	0.00	0.00	0.00	0.00	0.02	1.00	
0.00	0.00	0.00	-0.00	-0.00	-0.00	-0.00	0.02	0.96	1.00

Figure 6-21 : Cross-correlations Between Latitudes at the Backward Run

The asterisks in Figure 6-21 indicate the epochs at which coordinates are updated. Correlations between points of different legs are separated by dashed lines. The strong correlations are quite consistent with the pattern of the error curves shown in the last two sections. The errors in the filtered coordinates of the neighbouring points are

correlated in terms of magnitude and direction. The strong positive correlation means that, even though the absolute accuracies of the filtered coordinates are low, the relative accuracies between points which are short distances apart are still very high.

The control coordinates used in the filtering were considered as uncorrelated quantities, therefore all the correlations are the longest dashed line in Figure 6-21 are very small. They show that the correlation between points of different legs are negligible. Thus the same position determined in the forward and backward runs may be treated as uncorrelated quantities.

6.3.4 Initial State Vector

One of the unknown quantities in filtering is the initial state vector, x(o). Normally, the starting epoch (t = 0) of an inertial survey is the beginning of the first zero velocity update period at the first point of traverse. Since this period is only 30 seconds, the state vector at the end of this period, when the velocity update is performed, is a good approximation to the initial state vector. The optimal estimate of this state vector, $x_1^s(+)$ is obtained at the end of the optimal smoothing.

The results from the smoothing show that the initial misalignment of the vertical platform axis is much larger than that of the horizontal axes. The initial ε_U of the first two sets of data are approximately 100 and 90 arcsec, respectively, which is close to the 100 arcsec standard deviation that the author initially estimated.

The initial ε_U of the third set of data is about 30 arcsec, much smaller than the other two sets. The initial misalignments of the horizontal axes of the first surveys are less than the 5 arcsec standard deviation that the author used to estimate the initial variance matrix, but the ε_N of the second and third survey at the initial point are 8 and 9 arcsec, which perhaps explains the large change of the errors in the filtered longitudes in the third survey (>7 m in the backward run); see Figure 6-4.

These initial state vectors indicate that, in general, the initial assumptions on the variances are quite realistic. However, the 100 arcsec initial misalignment of the vertical axis is still too large. Since the filter requires at least two coordinate updates at different points on the traverse before it can obtain a reasonable estimate on the azimuth error, the azimuth-dependent errors in the first leg of the survey mission can only be controlled by improving the accuracy of the initial alignment.

Since there were large differences between the estimated standard deviations of the attitude errors and their initial values predicted by smoothing, the third set of FILS data was filtered and smoothed again using a new set of initial variances. The original initial variances given in Table 5-1 were modified such that they fit more closely the errors predicted for the initial state vector of the third survey. The modifications were 100" to 30" for ε_U and 5" to 9" for ε_N. The results show that the changes in the initial variances did not make any significant difference in the size and

pattern of the errors in the filtered and smoothed coordinates or their estimated variances. The changes in weighting were perhaps not large enough to bring any first order error changes to the estimated variances. The accuracies of the survey cannot be improved by varying the initial variances if they are reasonably accurate.

Chapter 7

CONCLUSIONS AND RECOMMENDATIONS

A Kalman filter-smoother for a local level inertial survey system (LLISS) has been developed in this research. It has two advantages over other estimation techniques available today. First, the filter-smoother estimates not only the systematic errors, i.e. state errors, in the LLISS but also their variances and covariances. Second, it accepts any measurement that can be expressed as a function of the state errors to improve its estimates. Although the estimation package has been designed for, and tested with the data collected by the Ferranti Inertial Land Surveyor (FILS), it can be easily modified to process data obtained from other local level inertial survey systems. The package utilizes the recursive Kalman filtering and backward smoothing equations. Thus, the filter may be used for real-time application and the large matrix inversions in the smoothing phase are avoided. The development of the optimal Kalman filter-smoother is divided into four major steps:

(i) the derivation of a dynamics matrix for the FILS from the general error equations;

(ii) the derivation of the analytical transition matrix from the dynamics matrix for error propagation;

(iii) implementation of the optimal Kalman filtering and backward smoothing equations for the estimation of the state errors in the FILS, and the

(iv) testing of the Kalman filter-smoother with the velocity and coordinate data gathered by a FILS.

Steps (i) and (ii) are more theoretical; therefore they are similar for all LLISS while the results of steps (iii) and (iv) are more dependent on the type of system used.

The first step involves the derivation of a set of differential equations which describe the time rate of change of the errors in the FILS. The general form of these equations is well documented. The special form of the dynamics matrix (given in Figure 3-1) to be used with the FILS was derived from these error equations. Its elements are the partial derivatives of the state errors with respect to other state errors. In this case, the 10×10 dynamics matrix was derived under the assumption that the system has been well calibrated. Thus, the state errors to be estimated are the 9 basic state errors and the residual drift rate of the vertical platform axis. The drift rate is included because results of calibrations indicate that it can be much larger than the residuals of the other two drift rates. Other constant instrument errors, e.g. drift rates and scale factors, can be included by extending the dynamics matrix. Such extensions may be necessary when the system is not well calibrated.

The second step, the derivation of the transition matrix has been accomplished by using the inverse Laplace transform technique. The derivation is a lengthy process, and it has to be repeated whenever the elements in the dynamics matrix are changed. Therefore it should only be used when the structure of the dynamics matrix is known. Otherwise, numerical techniques provide a higher degree of flexibility

in the derivation. The analytical approach was adopted in this case because it gives the analytical expressions for the influence of the individual state error on other state errors. These expressions are useful tools in the error analysis of an LLISS. Moreover, the expressions are less time consuming for generating the transition matrix than the numerical method, i.e. the truncated series expression approach, for propagation loop intervals ≥ 0.1 seconds.

In the third step, the major problem in the implementation of the Kalman filter-smoother is the selection of the initial variances of the state errors and their spectral variance density (see Chapter 5). In this case, the selection of the initial variances of the attitude errors and all the spectral variance densities were based on the experiences that the author gained by analyzing other LLISS. The initial variances for the coordinates and velocities were obtained by inspection of the survey data. Since these variances are normally updated with known coordinates and measured velocities at the beginning of the survey, their correctness is less critical than the variances for the attitude errors. Any selected set of variances must be finely tuned with actual data before they are acceptable for practical applications.

In the fourth step, tests were conducted with 3 data sets collected over a 42 km, L-shaped base line. The results after filtering indicated that, when only two end points are known, the maximum errors in the horizontal coordinates were less than 10 m and the maximum height error was below 4 m. The errors in latitudes

and longitudes were mostly azimuth dependent. Results after smoothing indicate that mean coordinates of a two way L-shaped survey with sub-metre 1σ accuracy can be obtained with a well calibrated system. When the corner point was treated as known, the results after filtering were more accurate in general and the error curves between known points became very linear. Errors in latitude and longitude were reduced to the 5 m range and the errors in the heights were less than 2 m. After smoothing, all errors were found to be at the metre range. The accuracies of the mean coordinates are better than 1 metre with the exception of a few longitudes in the first set of data. In general, the forward runs were less accurate than the backward runs,indicating that coordinate updates improved the accuracy of the predicted azimuths.

The variances generated by the filter and smoother were too pessimistic as compared to the actual errors. Further tests showed that they can be reduced to a more realistic level by selecting the spectral variance density of the horizontal and vertical velocities as $1.0 \cdot 10^{-6}\ m \cdot s^{-1}$ and $0.49\ \ 10^{-6}\ m \cdot s^{-1}$, respectively. Comparison between the selected initial standard deviation for the state errors and their actual values obtained from backward smoothing showed that the variances were quite realistic except for the attitude errors in the third set of data. There was no significant change in the results when this set of data was filtered and smoothed,again using a modified and less homogeneous set of initial variances. This indicates that changes in the initial variances do not bring any first-order

error changes to the estimated coordinates if the original variances are reasonably accurate. The variances given in Table 5-1 should be used for filtering until more tests with the FILS can be performed to obtain a better set of initial variances.

The cross-variances between the state errors at different points on the surveys were also computed. The correlations between the coordinates of the points between two coordinate updates were very strong and diminishing as the distance between the points increased. This showed that although the absolute errors in the coordinates are large, the relative accuracy between two positions determined by an LLISS is very high. When the coordinates were updated at a known point with uncorrelated control coordinates, the correlations between coordinates determined before and after the update vanish. This means that the coordinates of the same points in a two-way run with coordinate update at the end of the forward run can be treated as independent quantities. Comparison of the cross-variances with results of filtering showed that they are, in general, realistic. Therefore, they are important in the adjustment of a network of filtered coordinates (Schwarz and Gonthier, 1982). The effect of these correlations in such an adjustment needs further investigation.

The error model used in this research is based on the assumption that the gravity disturbances in the survey areas are small and do not change drastically from point to point. More research effort is needed to develop a refined gravity disturbance model for extending the filter to predict these errors. Another open question is the

derivation of a set of recursive equations for computing the cross-variances between smoothed state errors. These are important in inertial network adjustments that utilize the smoothed coordinates. Finally, the filter developed in this thesis can be modified for real-time application. The filter coordinates are accurate enough to maintain the linearity condition for the dynamic system. Since the filter can accept different types of measurements to improve the accuracy of the estimated state errors, it can be used to integrate the local level inertial survey system with other surveying systems. Examples are the aerial camera for photogrammetric mapping and the NAVSTAR/Global Positioning System in offshore positioning. The theoretical as well as the practical aspects of the integration and implementation of these hybrid systems need further investigations.

REFERENCES

Babbage, G., (1977), "Operation of the Inertial Survey System: the Manager's View", Proceedings of the First International Symposium on Inertial Technology for Surveying and Geodesy, Ottawa, October 1977.

Babbage, G., (1981), "Inertial Surveying - A Study in Accuracy and Versatility", Proceedings, The Second International Symposium on Inertial Technology for Surveying and Geodesy, June 1-5, 1981, Banff, Canada.

Bierman, G.J., (1973), "Fixed Interval Smoothing with Discrete Measurement", International Journal of Control, Vol. 18, No. 1.

Britting, K.R., (1971), Inertial Navigation System Analysis, Wiley-Interscience, New York.

Deren, G. and J. Hagglund, (1981), "Ferranti Mark II Survey Demonstration on the Defence Mapping Agency Wyoming Baseline", Technical Report, Sheltech, Canada.

Faddeev, D.K. and V.N. Faddeeva, (1963), Computational Methods of Linear Algebra, W.H. Freeman, San Francisco.

Gelb, A., (1974), Applied Optimal Estimation, The M.I.T. Press, Cambridge, Mass., Fourth printing, 1978.

Herrewegen, M.V.D., (1980), Practical Results With the FILS Inertial Surveyor, Institut Geographique National, Brussels.

Hochstadt, H., (1975), Differential Equations - A Modern Approach, Dover Publications, Inc., New York.

Kayton, M., (1961), "Fundamental Limitations on Inertial Measurements", Paper presented at the ARS Guidance, Control and Navigation Conference, Stanford, California, August 1961.

McCollum, P. and B. Brown, (1965), Laplace Transform Tables and Theorems, Holt, Rinehart and Winston Inc., N.Y.

Savage, P.G., (1978), "Strapdown Sensors", Strap-Down Inertial Systems, AGARD Lecture Series No. 95, 1978.

Schmidt, G.T., (1978), "Strapdown Inertial Systems - Theory and Applications - Introduction and Overview", AGARD Lecture Series No. 95.

Schwarz, K-P., (1978), "Accuracy of Vertical Deflection Determination by Present-Day Inertial Instrumentation", Proceedings, The 9th GEOP Conference, An International Symposium on the Applications of Geodesy to Geodynamics, October 2-5, 1978, Columbus, Ohio.

Schwarz, K-P., (1980a), "Inertial Surveying Systems - Experience and Prognosis", The Canadian Surveyor, Vol. 34, pp. 383-395.

Schwarz, K-P., (1980b), "Error Propagation in Inertial Positioning", The Canadian Surveyor, Vol. 34, No. 3, September, 1980.

Schwarz, K-P., (1980c), "Gravity Field Approximation Using Inertial Survey System", The Canadian Surveyor, Vol. 34, No. 4, December, 1980.

Schwarz, K-P and M. Gonthier (1982), "Adjustment Problems in Inertial Positioning", Proceedings of the International Symposium on Geodetic Networks and Computations of the IAG, Volume IV.

Sokolaikoff, I.S. and R.M. Redheffer, (1966), Mathematics of Physics and Modern Engineering, McGraw-Hill Book Co., New York.

Spiegel, M.R., (1968), Mathematical Handbook of Formulas and Tables, Schaum's Outline Series, McGraw-Hill Book Company, Toronto.

Vaníček, P. and E.J. Krakiwsky, (1982), Geodesy: The Concepts, North-Holland Publishing Co., New York.

Wong, V.C. and K-P. Schwarz, (1979), "Investigations on the Analytical Form of the Transition Matrix Inertial Geodesy", Technical Report No. 58, University of New Brunswick, Fredericton.

APPENDIX A

The step by step derivation of the attitude error equations is given in this appendix.

Given that

$$C_p^{\ell\ell} = I + E^{\ell\ell} \tag{3-6}$$

and

$$\dot{C}_p^{\ell\ell} = C_p^{\ell\ell}\, \Omega_{\ell\ell\, p}^{p}\,, \tag{3-20}$$

the time rate of change of the computed angular velocity between the platform and local level systems can be written as

$$\dot{\omega}_{\ell\ell\, p}^{\ell\ell} = (I + E)^{\ell\ell}\, \omega_{\ell\ell\, p}^{p} \tag{3-21}$$

The angular velocity $\omega_{\ell\ell\, p}^{\ell\ell}$ can be computed by the following steps

$$\begin{aligned}
\omega_{\ell\ell\, p}^{p} &= \omega_{ip}^{p} - \omega_{i\,\ell\ell}^{p} \\
&= \omega_{ip}^{p} - C_{\ell\ell}^{p}\, \omega_{i\,\ell\ell}^{\ell\ell} \\
&= \omega_{ip}^{p} - (I - E)^{\ell\ell}\, \omega_{i\,\ell\ell}^{\ell\ell} \\
&= \omega_{ip}^{p} - \omega_{i\,\ell\ell}^{\ell\ell} + E^{\ell\ell}\, \omega_{i\,\ell\ell}^{\ell\ell}
\end{aligned} \tag{A-1}$$

Also, the two angular velocities ω_{ip}^{p} and $\omega_{i\,\ell\ell}^{\ell\ell}$ may be expressed by

$$\omega_{i\,\ell\ell}^{\ell\ell} = \tilde{\omega}_{i\,\ell\ell}^{\ell\ell} - \delta\omega_{i\,\ell\ell}^{\ell\ell} \tag{A-2}$$

and

$$\omega_{ip}^{p} = \omega_{i\,\ell\ell}^{\ell\ell} + \delta\omega_{ip}^{p}\,. \tag{A-3}$$

The platform is torqued by the gyros to be aligned with the local level system, therefore the angular velocity difference between the two systems is the combined effect of the uncertainties in the gyros and the computed quantity $\tilde{\omega}^{\ell\ell}_{i\,\ell\ell}$. Equation (A-3) may be expanded to give

$$\begin{aligned}\omega^{p}_{ip} &= \omega^{\ell\ell}_{i\,\ell\ell} + \delta\omega^{p}_{ip} \\ &= \tilde{\omega}^{\ell\ell}_{i\,\ell\ell} + \delta d^{\ell\ell} + (u)\,\omega^{\ell\ell}_{i\,\ell\ell} \\ &= \omega^{\ell\ell}_{i\,\ell\ell} + \delta\omega^{\ell\ell}_{i\,\ell\ell} + \delta d^{\ell\ell} + (u)\,\omega^{\ell\ell}_{i\,\ell\ell} \quad . \end{aligned} \tag{A-4}$$

Substituting equation (A-1) into equation (A-4) after switching the position of $\omega^{\ell\ell}_{i\,\ell\ell}$ and $\omega^{p}_{\ell\ell\,p}$ yields

$$\omega^{\ell\ell}_{\ell\ell\,p} = E^{\ell\ell}\,\omega^{\ell\ell}_{i\,\ell\ell} + \delta\omega^{\ell\ell}_{i\,\ell\ell} + \delta d^{\ell\ell} + (u)\,\omega^{\ell\ell}_{i\,\ell\ell} \quad . \tag{A-5}$$

After substituting equation (A-5) into equation (3-21), the time rate of change of $\omega^{\ell\ell}_{\ell\ell\,p}$ becomes

$$\dot{\omega}^{\ell\ell}_{\ell\ell\,p} = (I+E)^{\ell\ell}\,(E^{\ell\ell}\omega^{\ell\ell}_{i\,\ell\ell} + \delta\omega^{\ell\ell}_{i\,\ell\ell} + \delta d^{\ell\ell}) + (u)\,\omega^{\ell\ell}_{i\,\ell\ell} \quad . \tag{A-6}$$

The products of the small angle matrices in equation (A-6) are second-order effects which can be eliminated in a first-order error analysis. Since the attitude error $\varepsilon^{\ell\ell}$ is the only time dependent quantity in $\omega^{\ell\ell}_{\ell\ell\,p}$, the attitude error equation may be rewritten as

$$\dot{\varepsilon}^{\ell\ell} = -\Omega^{\ell\ell}_{i\,\ell\ell}\,\varepsilon^{\ell\ell} + \delta\omega^{\ell\ell}_{i\,\ell\ell} + \delta d^{\ell\ell} + (u)\,\omega^{\ell\ell}_{i\,\ell\ell} \quad . \tag{3-23}$$

Using the components of $\omega^{\ell\ell}_{i\,\ell\ell}$

$$\omega^{\ell\ell}_{i\,\ell\ell} = \{-\dot{\phi},\ \ell\cos\phi,\ \ell\sin\phi\}^T \quad , \tag{2-3}$$

the following matrix is formed:

$$\Omega^{\ell\ell}_{i\,\ell\ell} = -\begin{bmatrix} 0 & \ell\sin\phi & -\ell\cos\phi \\ -\ell\sin\phi & 0 & -\dot{\phi} \\ \ell\cos\phi & \dot{\phi} & 0 \end{bmatrix} \quad . \tag{2-10}$$

Substituting (3-24) and (2-10) into equation (3-23) the attitude error equation in matrix form becomes

$$\begin{bmatrix} \dot{\varepsilon}_E \\ \dot{\varepsilon}_N \\ \dot{\varepsilon}_U \end{bmatrix} = \begin{bmatrix} 0 & \ell\sin\phi & \ell\cos\phi & 0 & 0 & -1 & 0 \\ -\ell\sin\phi & 0 & -\dot{\phi} & -\ell\sin\phi & 0 & 0 & \cos\phi \\ \ell\cos\phi & \dot{\phi} & 0 & \ell\cos\phi & 0 & 0 & \sin\phi \end{bmatrix} \begin{bmatrix} \varepsilon_E \\ \varepsilon_N \\ \varepsilon_U \\ \delta\phi \\ \delta\lambda \\ \delta\dot{\phi} \\ \delta\dot{\lambda} \end{bmatrix}$$

$$+ \delta d^{\ell\ell} + (u)\ \omega^{\ell\ell}_{i\,\ell\ell} \quad . \tag{3-25}$$

APPENDIX B

The different terms in the acceleration error equations for a local level inertial survey system are derived here.

From equation (2-7) and (2-8) we can write the second term in equation (3-16) as

$$(\Omega^{\ell\ell}_{e\,\ell\ell} + 2\Omega^{\ell\ell}_{ie})\, V^{\ell\ell} = -\begin{bmatrix} -r(\dot{\lambda}+2\omega_e)\sin\phi & 0 & (\dot{\lambda}+2\omega_e)\cos\phi \\ 0 & \frac{r}{2}(\dot{\lambda}+2\omega_e)\sin 2\phi & \dot{\phi} \\ -r\,\dot{\phi} & r(\dot{\lambda}+2\omega_e)\cos^2\phi & 0 \end{bmatrix} \begin{bmatrix} \delta\dot{\phi} \\ \delta\dot{\lambda} \\ \delta\dot{h} \end{bmatrix} \tag{B-1}$$

Premultiplying the skew-symmetric matrix of $V^{\ell\ell}$

$$V^{\ell\ell} = \begin{bmatrix} 0 & -V_U & V_N \\ V_U & 0 & -V_E \\ -V_N & V_E & 0 \end{bmatrix} \tag{B-2}$$

into the sum $(\delta\omega^{\ell\ell}_{e\,\ell\ell} + 2\,\delta\omega^{\ell\ell}_{ie})$, the third term is obtained:

$$V^{\ell\ell}(\delta\omega^{\ell\ell}_{e\,\ell\ell} + 2\delta\omega^{\ell\ell}_{ie}) = \begin{bmatrix} (\dot{\lambda}+2\omega_e)(V_U\sin\phi + V_N\cos\phi) & 0 & 0 & -V_U\cos\phi + V_N\sin\phi \\ -(\dot{\lambda}+2\omega_e)V_E\cos\phi & 0 & -V_U & -V_E\sin\phi \\ (\lambda+2\omega_e)V_E\sin\phi & 0 & V_N & V_E\cos\phi \end{bmatrix} \begin{bmatrix} \delta\phi \\ \delta\lambda \\ \delta\dot{\phi} \\ \delta\dot{\lambda} \end{bmatrix} \tag{B-3}$$

After eliminating all the products of velocities (see section 3.2.2 for explanation) and rewriting every term in equation (B-3) in geodetic curvilinear coordinates, the equation becomes

$$V^{\ell\ell}(\delta\omega^{\ell\ell}_{e\,\ell\ell} + 2\,\delta\omega^{\ell\ell}_{i\,e}) = \begin{bmatrix} 0 & 0 & 0 & \dot{\phi}\tan\phi - \frac{\dot{h}}{r} \\ 0 & 0 & -\frac{\dot{h}}{r} & -\frac{1}{2}\dot{\lambda}\sin 2\phi \\ 0 & 0 & r\dot{\phi} & r\,\dot{\lambda}\cos^2\phi \end{bmatrix} \begin{bmatrix} \delta\phi \\ \delta\lambda \\ \delta\dot{\phi} \\ \delta\dot{\lambda} \end{bmatrix} . \qquad (3\text{-}27)$$

Substituting equations (3-15), (B-1) and (3-28) into equation (3-16) and assuming that $V^{\ell\ell} << 2\omega_e$, the acceleration error equations may be written as

$$\begin{bmatrix} \delta\ddot{\phi} \\ \delta\ddot{\lambda} \\ \delta\ddot{h} \end{bmatrix} = \begin{bmatrix} \frac{fU}{r} & 0 & -\frac{fE}{r} & 0 & 0 & 0 & -\ell\sin 2\phi & 0 & -\frac{2\dot{\phi}}{r} \\ 0 & \frac{-fU\sec\phi}{r} & \frac{fN\sec\phi}{r} & 0 & 0 & 2\ell\tan\phi & 0 & 0 & \frac{-(\dot{\lambda}+2\omega_e)}{r} \\ -fN & fE & 0 & 0 & 0 & 2r\dot{\phi} & 2r\ell\cos^2\phi & \frac{2\gamma(1-\alpha)}{r} & 0 \end{bmatrix} \begin{bmatrix} \varepsilon_E \\ \varepsilon_N \\ \varepsilon_U \\ \delta\phi \\ \delta\lambda \\ \delta\dot{\phi} \\ \delta\dot{\lambda} \\ \delta h \\ \delta\dot{h} \end{bmatrix}$$

$$+ \begin{bmatrix} \xi\gamma \\ \eta\gamma \\ \Delta g \end{bmatrix} + (\Delta\, C_a^p)^T\, f^{\ell\ell} + S_a f^a + (u)\, f^a \; . \qquad (3\text{-}29)$$

APPENDIX C

The analytical expressions for elements in the transition matrix of the ten state errors for a small time interval t are given below:

$$\Phi(1,1) = \cos\mu t$$

$$\Phi(1,2) = \ell t \sin\phi \cos\mu t$$

$$\Phi(1,3) = \frac{fe}{\mu^2}(\cos\ell t - \cos\mu t) - \frac{\ell}{\mu}\cos\phi\,(\sin\mu t - \frac{\ell}{\mu}\sin\ell t)$$

$$\Phi(1,4) = \frac{\ell^2}{\mu^2}(\cos\mu t - \cos\ell t)(1 - 2\sin^2\phi) - \frac{\ell^2 t}{\mu}\sin^2\phi\,\sin\mu t$$

$$\Phi(1,5) = 0$$

$$\Phi(1,6) = \frac{-\sin\mu t}{\mu}$$

$$\Phi(1,7) = \frac{\ell t}{2\mu}\sin 2\phi\,\sin\mu t + \frac{fe}{2\mu^3}\sin\phi\,(\sin\mu t - \mu t\cos\mu t)$$

$$\Phi(1,8) = \frac{2\zeta}{r}(\dot{\phi}\,ek2 - \ell^2\sin 2\phi\,su1)$$

$$\Phi(1,9) = \frac{2}{r}(\dot{\phi}\,ek1 - \ell^2\sin 2\phi\,su2)$$

$$\Phi(1,10) = \frac{fe}{\mu^2}(\frac{\sin\ell t}{\ell} - \frac{\sin\mu t}{\mu})$$

$$\Phi(2,1) = \sin\phi\,[\ell t\,(1 - \cos\mu t) - \sin\ell t]$$

$$\Phi(2,2) = \cos\mu t$$

$$\Phi(2,3) = (\frac{fn}{\mu^2} - \frac{\ell^2\sin 2\phi}{2\mu^2})(\cos\ell t - \cos\mu t) + \frac{\ell^2 t}{2\mu}\sin 2\phi\,\sin\mu t$$

$$\Phi(2,4) = \frac{\ell}{\mu}\sin\phi\,(\frac{\ell}{\mu}\sin\ell t - \sin\mu t)$$

$\Phi(2,5) = 0$

$\Phi(2,6) = \frac{\ell t}{\mu} \sin\phi \sin\mu t$

$\Phi(2,7) = \frac{\cos\phi \sin\mu t}{\mu}$

$\Phi(2,8) = \frac{\zeta\ell}{r} (4\dot{\phi} \sin\phi \, su1 + 2\cos\phi \, ek2)$

$\Phi(2,9) = \frac{-\ell}{r} (4\dot{\phi} \sin\phi \, su2 + 2\cos\phi \, ek1)$

$\Phi(2,10) = \sigma(t)$

$\Phi(3,1) = \sec\phi \, (\sin\ell t - \ell t \sin^2\phi \cos\mu t)$

$\Phi(3,2) = \tan\phi \, (\cos\mu t - \cos\ell t)$

$\Phi(3,3) = \cos\ell t$

$\Phi(3,4) = \sec\phi \, (\sin\ell t - \frac{\ell}{\mu} \sin^2\phi \sin\mu t)$

$\Phi(3,5) = 0$

$\Phi(3,6) = \tan\phi \, \Phi(2,6)$

$\Phi(3,7) = \frac{\sin\phi \sin\mu t}{\mu}$

$\Phi(3,8) = \tan\phi \, \Phi(2,8)$

$\Phi(3,9) = \tan\phi \, \Phi(2,9)$

$\Phi(3,10) = \frac{\sin\ell t}{\ell}$

$\Phi(4,1) = \cos\ell t - \cos\mu t$

$\Phi(4.2) = \sin\phi \, (\sin\ell t - \ell t \cos\mu t)$

$$\Phi(4,3) = \frac{-fe}{\mu^2}(\cos\ell t - \cos\mu t) - \cos\phi\ (\sin\ell t - \frac{\ell}{\mu}\sin\mu t)$$

$$\Phi(4,4) = \cos\ell t$$

$$\Phi(4,5) = 0$$

$$\Phi(4,6) = \frac{\sin\mu t}{\mu}$$

$$\Phi(4,7) = -\Phi(1,7)$$

$$\Phi(4,8) = -\Phi(1,8)$$

$$\Phi(4,9) = -\Phi(1,9)$$

$$\Phi(4,10) = \frac{-fe}{\mu^2}(\frac{\sin\ell t}{\ell} - \frac{\sin\mu t}{\mu})$$

$$\Phi(5,1) = \ell fn(ul0 + 2\ su2) + \ell\mu^2\ \tan\phi\ (ul0 + 2\ uu0)$$

$$\Phi(5,2) = \sec\phi\ (\cos\mu t - \cos^2\phi - \sin^2\phi\ \cos\ell t)$$

$$\Phi(5,3) = \frac{fn\ \sec\phi}{\mu^2}(\cos\ell t - \cos\mu t) - \sin\phi\ (1 - \cos\ell t - \frac{\ell^2 t}{\mu}\sin\mu t)$$

$$\Phi(5,4) = \frac{\ell}{\mu^2}(\mu^2\ \tan\phi + fn)(\frac{\sin\ell t}{\ell} - \frac{\sin\mu t}{\mu})$$

$$\Phi(5,5) = 1$$

$$\Phi(5,6) = \sec\phi\ \Phi(2,6)$$

$$\Phi(5,7) = \sec\phi\ \Phi(2,7)$$

$$\Phi(5,8) = \sec\phi\ \Phi(2,8)$$

$$\Phi(5,9) = \sec\phi\ \Phi(2,9)$$

$$\Phi(5,10) = \sec\phi\ \frac{fn}{\mu^2}(\frac{\sin\ell t}{\ell} - \frac{\sin\mu t}{\mu})$$

$$\Phi(6,1) = \mu \sin\mu t + \ell \sin^2\phi(\sin\ell t - \frac{\ell}{\mu}\sin\mu t) - \frac{fe}{\mu^2}\ell\cos\phi(\cos\ell t - \cos\mu t)$$

$$\Phi(6,2) = \ell \sin\phi(\cos\ell t - \cos\mu t + \mu t \sin\mu t)$$

$$\Phi(6,3) = \frac{fn}{2\mu}\ell t \sin\phi \sin\mu t - \frac{fe}{\mu}(\sin\mu t - \frac{\ell}{\mu}\sin\ell t) - \ell\cos\phi(\cos\ell t - \cos\mu t - 2\mu^2\ell^2\sin^2\phi\ u122)$$

$$\Phi(6,4) = \frac{\ell}{\mu}(\ell \sin\mu t - \mu \sin\ell t) - \frac{fe}{\mu^2}\ell\cos\phi(\cos\ell t - \cos\mu t) + \frac{\ell^2}{2\mu^3}\sin 2\phi\ (\mu^2\tan\phi + fn)(\sin\mu t - \mu t\cos\mu t)$$

$$\Phi(6,5) = 0$$

$$\Phi(6,6) = \cos\mu t$$

$$\Phi(6,7) = \frac{\ell}{\mu}\sin\phi\cos\phi(\sin\mu t + \mu t\cos\mu t) - \frac{fe}{2\mu}t\sin\phi\sin\mu t$$

$$\Phi(6,8) = \frac{-2\zeta}{r}(\dot{\phi}\ ek1 - \ell^2\sin 2\phi\ su2)$$

$$\Phi(6,9) = \frac{-2}{r}(\dot{\phi}\ eu2 - \ell^2\sin 2\phi\ su3)$$

$$\Phi(6,10) = \frac{fe}{\mu^2}(\cos\mu t - \cos\ell t)$$

$$\Phi(7,1) = \frac{fn}{\mu^2}\ell(\cos\ell t - \cos\mu t + 2\mu^2\ su3) + \ell\tan\phi(\cos\ell t - \cos\mu t + \mu t\sin\mu t)$$

$$\Phi(7,2) = -\mu\sec\phi\left[\sin\mu t + \frac{\ell}{\mu}\sin^2\phi(\sin\ell t - \frac{\ell}{\mu}\sin\mu t)\right]$$

$$\Phi(7,3) = \frac{fn}{\mu^2}\sec\phi(\mu\sin\mu t - \ell\sin\ell t) + \ell\sin\phi(\ell t\cos\mu t - \sin\ell t) - \frac{fe}{2\mu}\ell t\cos\phi\sin\mu t$$

$$\Phi(7,4) = \frac{\ell}{\mu^2}(\mu^2\tan\phi + fn)(\cos\ell t - \cos\mu t)$$

$\Phi(7,5) = 0$

$\Phi(7,6) = \frac{\ell}{\mu} \tan\phi \ (\sin\mu t + \mu t \cos\mu t)$

$\Phi(7,7) = \cos\mu t$

$\Phi(7,8) = \frac{-2\zeta}{r} \ (\ell \ ek1 + 2\dot{\phi}\ell \tan\phi \ su2)$

$\Phi(7,9) = \frac{-2}{r} \ (\ell \ eu2 + 2\dot{\phi}\ell \tan\phi \ su3)$

$\Phi(7,10) = \frac{fn}{\mu^2} \sec\phi \ (\cos\ell t - \cos\mu t)$

$\Phi(8,1) = r(2\dot{\phi}\mu^2 \ el2 - fn \ el3 - fe \ \mu^2\ell \sin\phi \ el0)$

$\Phi(8,2) = r[fe \ el3 + \ell \ el2 \ (fn \sin\phi - 2\mu^2 \cos\phi)]$

$\Phi(8,3) = r(3 \ fn \ \ell \cos\phi \ el2 - 2 \ fe \ \dot{\phi} \ el2)$

$\Phi(8,4) = r(\mu^2\ell^2 \sin2\phi \ el1 - fe \ \ell \sin\phi \ el2)$

$\Phi(8,5) = 0$

$\Phi(8,6) = r(2\dot{\phi} \ ek1 + fn \ ek2 + 2\ell^2 \sin2\phi \ su2)$

$\Phi(8,7) = r(2\ell \cos^2\phi \ ek1 + fe \cos\phi \ ek2 - 2\dot{\phi}\ell \sin2\phi \ su2)$

$\Phi(8,8) = \cosh \sqrt{\zeta} \ t$

$\Phi(8,9) = \frac{\sinh \sqrt{\zeta} \ t}{\sqrt{\zeta}}$

$\Phi(8,10) = \sigma(t)$

$\Phi(9,1) = r(2\dot{\phi}\mu^2 \ el3 - fe\mu^2 \ \ell \sin\phi \ el2 - fn \ el4)$

$\Phi(9,2) = r[fe\ el4 + \ell\ el3\ (fn\ \sin\phi - 2\ \mu^2\ \cos\phi)]$

$\Phi(9,3) = r(3fn\ \ell\ \cos\phi\ el3 - 2fe\ \dot{\phi}\ el3)$

$\Phi(9,4) = r(\mu^2\ell^2\ \sin2\phi\ el2 - fe\ \ell\ \sin\phi\ el3)$

$\Phi(9,5) = 0$

$\Phi(9,6) = r(2\dot{\phi}\ eu2 + fn\ ek1 + 2\ell^2\ \sin2\phi\ su3)$

$\Phi(9,7) = r(2\ell^2\ \cos^2\phi\ eu2 + fe\ \cos\phi\ ek1 - 2\dot{\phi}\ \ell\ \sin2\phi\ su3)$

$\Phi(9,10) = \sigma(t)$

$\Phi(10,1) = 0$

$\Phi(10,2) = 0$

$\Phi(10,3) = 0$

$\Phi(10,4) = 0$

$\Phi(10,5) = 0$

$\Phi(10,6) = 0$

$\Phi(10,7) = 0$

$\Phi(10,8) = 0$

$\Phi(10,9) = 0$

$\Phi(10,10) = 1$

where

$$fe = \frac{fE}{r}$$

$$fn = \frac{fN}{r}$$

$$\zeta = 2\mu^2 - k_2$$

$$ul0 = \frac{1}{\mu^2}\left(\frac{\sin\ell t}{\ell} - \frac{\sin\mu t}{\mu}\right)$$

$$uu0 = \frac{1}{2\mu^3}\left(\sin\mu t - \mu t\cos\mu t\right)$$

$$ul22 = \frac{\sin\mu t + \sin\ell t}{4\mu\ (\mu+\ell)^2} - \frac{t}{2\mu^2}\cos\mu t + \frac{\sin\mu t - \sin\ell t}{4\mu\ (\mu-\ell)^2}$$

$$ek1 = \frac{1}{a-b}\left[\frac{\mu\sin\mu t - a(\cos\mu t - e^{at})}{a^2+\mu^2} - \frac{\mu\sin\mu t - b(\cos\mu t - e^{bt})}{b^2+\mu^2}\right]$$

$$ek2 = \frac{1}{\mu(a-b)}\left[\frac{\mu(\cos\mu t - e^{bt}) + b\sin\mu t}{(b^2+\mu^2)} - \frac{\mu(\cos\mu t - e^{at}) + a\sin\mu t}{(a^2+\mu^2)}\right]$$

$$eu2 = \frac{1}{a-b}\left[\frac{a\mu\sin\mu t - a^2(\cos\mu t - e^{at})}{a^2+\mu^2} - \frac{b\mu\sin\mu t - b^2(\cos\mu t - e^{bt})}{b^2+\mu^2}\right]$$

$$sul = \frac{1}{2\mu(a-b)}\left[\frac{t(b\sin\mu t + \mu\cos\mu t)}{b^2+\mu^2} + \frac{(b^2-\mu^2)\sin\mu t + 2b\mu(\cos\mu t - e^{bt})}{(b^2+\mu^2)^2}\right.$$

$$\left. - \frac{t(a\sin\mu t + \mu\cos\mu t}{a^2+\mu^2} - \frac{(a^2-\mu^2)\sin\mu t + 2a\mu(\cos\mu t - e^{at})}{(a^2+\mu^2)^2}\right]$$

$$su2 = \frac{1}{2\mu(a-b)}\left\{b\left[\frac{t(b\sin\mu t - \mu\cos\mu t}{b^2+\mu^2} + \frac{(b^2-\mu^2)\sin\mu t + 2b\mu(\cos\mu t - e^{bt})}{(b^2+\mu^2)^2}\right]\right.$$

$$\left. -a\left[\frac{t(a\sin\mu t - \mu\cos\mu t)}{a^2+\mu^2} + \frac{(a^2-\mu^2)\sin\mu t + 2a\mu(\cos\mu t - e^{at})}{(a^2+\mu^2)^2}\right]\right\}$$

$$su3 = \frac{1}{2\mu(a-b)}\{[\frac{\mu t(-\mu \sin\mu t + a\cos\mu t) + a\sin\mu t + \mu\cos\mu t}{a^2 + \mu^2}$$

$$+ \frac{\mu(a^2-\mu^2)\cos\mu t - 2a\mu^2 \sin\mu t - 2a^2\mu e^{-at}}{(a^2+\mu^2)^2}]a$$

$$- [\frac{\mu t(b\cos\mu t - \mu\sin\mu t) + b\sin\mu t + \mu\cos\mu t}{(b^2+\mu^2)}$$

$$- \frac{\mu(b^2-\mu^2)\cos\mu t - 2b\mu^2\sin\mu t - 2b^2\mu e^{-bt}}{(b^2+\mu^2)^2}]b\}$$

$$el1 = \frac{1}{\mu^2(a-b)}[\frac{\mu\sin\mu t - b(\cos\mu t - e^{bt})}{b^2+\mu^2} - \frac{\ell\sin\ell t - b(\cos\ell t - e^{bt})}{b^2+\ell^2}$$

$$- \frac{\mu\sin\mu t - a(\cos\mu t - e^{at})}{a^2+\mu^2} + \frac{\ell\sin\ell t - a(\cos\ell t - e^{at})}{a^2+\ell^2}$$

$$el2 = \frac{1}{\mu^2(a-b)}[\frac{\mu b\sin\mu t + \mu^2(\cos\mu t - e^{bt})}{b^2+\mu^2} - \frac{\ell b\sin\ell t + \ell^2(\cos\ell t - e^{bt})}{b^2+\ell^2}$$

$$- \frac{\mu a\sin\mu t + \mu^2(\cos\mu t - e^{at})}{a^2+\mu^2} + \frac{\ell a\sin\ell t + \ell^2(\cos\ell t - e^{at})}{a^2+\ell^2}$$

$$el3 = \frac{1}{\mu^2(a-b)}\{b[\frac{\mu b\sin\mu t + \mu^2(\cos\mu t - e^{bt})}{b^2+\mu^2} - \frac{\ell b\sin\ell t + \ell^2(\cos\ell t - e^{bt})}{b^2+\ell^2}]$$

$$- a[\frac{\mu a\sin\mu t + \mu^2(\cos\mu t - \ell^{at})}{a^2+\mu^2} + \frac{\ell a\sin\ell t + \ell^2(\cos\ell t - e^{at})}{a^2+\ell^2}]\}$$

$$el4 = \frac{b(\mu\sin\mu t - b(\cos\mu t - e^{bt}))}{(a-b)(\mu^2+b^2)} - \frac{\ell(b\sin\ell t + \ell(\cos\ell t - e^{bt}))}{(a-b)(\ell^2+\mu^2)}$$

$$- \frac{a(\mu\sin\mu t - a(\cos\mu t - e^{at}))}{(a-b)(\mu^2+a^2)} + \frac{\ell(a\sin\ell t + \ell(\cos\ell t - e^{at}))}{(a-b)(\ell^2+\mu^2)}$$

$a = \sqrt{\zeta}$

$b = -\sqrt{\zeta}$

APPENDIX D

The analytical expression for the elements in the Q matrix can be derived from equation (5-7). Many of the values of these elements are relatively constant and very small over a small time interval t, therefore some of the complex integrations of the higher order terms are assumed negligible in this research. The elements of the upper triangle of Q in the filter are:

$$Q(1,1) = q1(0.5t + \frac{\sin 2\mu t}{4\mu}) + \frac{q6}{\mu^2}(0.5t - \frac{\sin 2\mu t}{4\mu})$$

$$Q(1,3) = q7 \sin 2\phi \frac{q7}{2\mu^2} \sin 2\phi (0.5t - \frac{\sin 2\mu t}{4\mu})$$

$$Q(1,4) = q1 \frac{\sin \mu t}{\mu} - Q(1,1)$$

$$Q(1,6) = (q\,1\mu - \frac{q6}{\mu}) \frac{\sin^2 \mu t}{2\mu}$$

$$Q(1,8) = -r\ q1\ fn\ ce13$$

$$Q(1,9) = -r\ q1\ fn\ ce14$$

$$Q(2,2) = q1(0.5t + \frac{\sin 2\mu t}{4\mu}) + \frac{q7}{\mu^2} \sec^2\phi (0.5t - \frac{\sin 2\mu t}{4\mu})$$

$$Q(2,5) = \sec\phi [q1(0.5t + \frac{\sin 2\mu t}{4\mu} - \frac{\sin \mu t}{\mu}) + \frac{q7}{\mu^2} \cos^2\phi (0.5t - \frac{\sin 2\mu t}{4\mu})]$$

$$Q(2,7) = \left(\frac{q7}{\mu}\cos\phi - q1\,\mu\,\sec\phi\right)\frac{\sin^2\mu t}{2\mu}$$

$$Q(2,8) = r\ fe\ q2\ cel3$$

$$Q(2,9) = r\ fe\ q2\ cel4$$

$$Q(3,3) = q3\left(\frac{\sin 2\ell t}{4\ell} + 0.5t\right) + \frac{q7}{\mu^2}\sin\phi\ \sin\phi\,(0.5t - \frac{\sin 2\mu t}{4\mu})$$

$$Q(3,4) = \frac{-fe}{\mu^2}\,q3\left[\frac{\sin t}{\ell} - \frac{\sin\mu t\ \sin\ell t}{\mu} + \frac{\ell}{\mu^2}\,(1 - \cos\mu t\ \cos\ell t)\right]$$

$$+ \frac{q6}{\mu^2}\,\ell t(0.5t - \frac{\sin 2\mu t}{4\mu})$$

$$Q(3,5) = \frac{fn}{\mu^2}\,q3\ fn\ \sec\phi\left[\frac{\sin\ell t}{\ell} - \frac{\sin\mu t\ \sin\ell t}{\mu} + \frac{\ell}{\mu^2}\,(1 - \cos\mu t\ \cos\ell t)\right]$$

$$+ \frac{q7}{\mu^2}\,\sin\phi\,(0.5t - \frac{\sin 2\mu t}{\mu})$$

$$Q(3,6) = q6\ \ell t\ \sin\phi\ \tan\phi\ \frac{\sin^2\mu t}{2\mu^2} - \frac{fe}{\mu^2}\,q3(\cos\ell t - \cos\mu t)$$

$$Q(3,7) = \frac{fn}{\mu^2}\,q3(\cos\ell t - \cos\mu t) + q7\ \sin\phi\ \frac{\sin^2\mu t}{2\mu^2}$$

$$Q(4,4) = \frac{q6}{\mu^2}\,(0.5t - \frac{\sin 2\mu t}{4\mu}) + (q1 + q3\,\frac{fe^2}{\mu^4})\ (1.5t - \frac{2\ \sin\mu t}{\mu}$$

$$+ \frac{\sin 2\mu t}{4\mu})$$

$$Q(4,6) = q6\ \frac{\sin^2\mu t}{2\mu^2} + (q1 + q3\,\frac{fe^2}{\mu^4})\ (1 - \cos\mu t - 0.5\ \sin^2\mu t)$$

$$Q(5,5) = \frac{q7}{\mu^2}(0.5t - \frac{\sin 2\mu t}{4\mu}) + \sec^2\phi(q2 + q3\frac{fn^2}{\mu^4})(1.5t - \frac{2\sin\mu t}{\mu} + \frac{\sin 2\mu t}{4\mu})$$

$$Q(5,7) = \frac{q7\sin^2\mu t}{\mu^2} - \sec^2\phi(q2 - q3\frac{fn^2}{\mu^2})(1 - \cos\mu t - 0.5\sin^2\mu t)$$

$$Q(6,6) = q6(\frac{\sin 2\mu t}{4\mu} + 0.5t) + \mu^2(q1 + q3\frac{fe^2}{\mu^4})(0.5t - \frac{\sin 2\mu t}{4\mu})$$

$$Q(6,7) = \ell(2\,q6\tan\phi - q7\sin 2\phi)\frac{\sin^2\mu t}{2\mu^2}$$

$$Q(7,7) = q7(0.5t + \frac{\sin 2\mu t}{4\mu}) + \mu^2\sec\phi(q2 + q3\frac{fn^2}{\mu^4})(0.5t - \frac{\sin 2\mu t}{4\mu})$$

$$Q(8,8) = q9(\frac{e^{2at} - e^{2bt} - 4at}{2a(a-b)(a-b)})$$

$$Q(8,9) = q9(\frac{e^{2at} - 2e^{(a+b)t} + e^{2bt}}{2(a-b)(a-b)})$$

$$Q(9,9) = q9\,a(\frac{e^{2at} + 4at - e^{2bt}}{2(a-b)(a-b)})$$

where

q1, q2, ... q9 are the diagonal elements

$\bar{Q}(1,1)$, $\bar{Q}(2,2)$, ... $\bar{Q}(9,9)$

$$ce13 = b\frac{b\,csut + \mu(ccut - cx2)}{\mu(a-b)(b^2+\mu^2)} + b\ell\frac{b\,cslt + \ell(cclt - cl2)}{\mu^2(a-b)(b^2+\mu^2)} + a\ell\frac{a\,cslt + (cclt - cll)}{\mu^2(a-b)(a^2+\mu^2)} - a\frac{a\,csut + \mu(ccut - cxl)}{\mu(a-b)(a^2+\mu^2)}$$

$$cel4 = \frac{a}{a-b}\left[\frac{\mu\ cs\mu t - a(ccut - cx1)}{(a^2 + \mu^2)} - \left(\frac{\ell}{\mu}\right)^2 \frac{\ell\ cslt - a(cclt - c11)}{(a^2 + \ell^2)}\right]$$

$$- \frac{b}{a-b}\left[\frac{\mu\ cs\mu t - b(ccut - cx2)}{(b^2 + \mu^2)} - \left(\frac{\ell}{\mu}\right)^2 \frac{\ell\ cslt - b(cclt - c12)}{(b^2 + \ell^2)}\right]$$

$$ccut = 0.5t + \frac{\sin 2\mu t}{4\mu}$$

$$csut = \frac{\sin^2 \mu t}{2\mu}$$

$$cslt = \frac{\sin\mu t \sin\ell t}{\mu} + \frac{\ell}{\mu^2}(1 - \cos\mu t \cos\ell t)$$

$$cclt = \frac{\cos\ell t \sin\mu t}{\mu} - \frac{\ell}{\mu^2}\sin\ell t \cos\mu t$$

$$cx1 = \frac{e^{at}(a\cos\mu t + \mu \sin\mu t) - a}{a^2 + \mu^2}$$

$$cx2 = \frac{e^{bt}(b\cos\mu t + \mu \sin\mu t) - b}{b^2 + \mu^2}$$

$$c11 = \frac{e^{at}(a\cos\ell t + \ell \sin\ell t) - a}{a^2 + \ell^2}$$

and

$$c12 = \frac{e^{bt}(b\cos\ell t + \ell \sin\ell t) - b}{b^2 + \ell^2}$$

All other elements in the upper triangle of the Q matrix are assumed to be zero because they are relatively constant and very small.

APPENDIX E

Due to the simple structure of the design matrix used in zero velocity and coordinate updates, the gain matrix may be computed by the equation

$$K(i, 1) = P(i, j) / (P(j, j) + R) \qquad (5\text{-}15)$$

when the observations are considered as uncorrelated quantities and are used one at a time to update the filter estimates. In this appendix, an example is used to explain the formulation of equation (5-15).

Assume that the velocity $\dot{\phi}$ is observed at a vehicle stop. This observed velocity is equal to the state error $\delta\dot{\phi}$ because the vehicle is not moving with respect to the earth. Thus the observation

$$\dot{\phi} = \delta\dot{\phi} + y \ , \qquad (E\text{-}1)$$

where y is the measurement noise, and the design matrix

$$H = [0 \quad 0 \quad 0 \quad 0 \quad 0 \quad 1 \quad 0 \quad 0 \quad 0 \quad 0] \ . \qquad (E\text{-}2)$$

The quantity

$$HPH^T = P(6, 6) \ , \qquad (E\text{-}3)$$

and the i^{th} element of the vector PH^T is

$$PH^T (i, 1) = P(i, 6) \ . \qquad (E\text{-}4)$$

Let R be the variance of the observed $\dot{\phi}$ and substituting equations (E-3) and (E-5) in equation (5-6), it becomes obvious that the i^{th}

element of the gain matrix (vector in this case)

$$K(i, 1) = P(i, j)\ (P(6, 6) + R)^{-1} \qquad \text{(E-5)}$$

or

$$K(i, 1) = P(i, j) / (P(j, j) + R) \qquad \text{(5-15)}$$

for $j = 6$.

The other two observed $\dot{\lambda}$ and $\dot{h}$ can be used to update the filter estimate in the same way by setting

$$j = 7 , \qquad \text{(E-7)}$$

and

$$j = 9 . \qquad \text{(E-9)}$$

This approach can replace the update procedure that uses the full gain matrix, i.e. a 10 × 3 matrix, by 3 separate velocity updates with a (10, 1) gain vector each. Since the velocities are observed at the same time, the transition matrices between the 3 separate velocity updates are unit matrices. The main objective of this approach is to avoid the matrix inversion in equation (5-6) so that the filter can process a larger number of observations for less strain on the computer.